

Special issue in honour of Prof. Reto J. Strasser

REVIEW

Revisiting JIP-test: An educative review on concepts, assumptions, approximations, definitions and terminology

M. TSIMILLI-MICHAEL

3 Ath. Phylactou, Nicosia CY-1100, Cyprus

Abstract

The aim of this educative review is, by revisiting the JIP-test as introduced and further elaborated and extended by Professor Reto J. Strasser and his research group, to clarify concepts, assumptions, and approximations on which it is based, as well as definitions and terms it uses, reminding that it is meant to evaluate impacts of environmental stresses – factors and/or perturbations – on the photosynthetic structure and function. It analyses how the JIP-test, based on the Theory of Energy Fluxes and adopting Duysens' concept, translates the OJIP polyphasic chlorophyll *a* fluorescence rise kinetics, emitted by PSII, into biophysical parameters to be compared. The interpretation of the OJIP sequential steps and in-between phases, the definitions/meanings and formulae derivations of quantum yields, probabilities, efficiencies, specific energy fluxes, inactive PSII reaction centres, and performance indexes (PI_{ABS} , PI_{total}) is addressed in detail. OJIP normalizations and subtractions providing semiquantitative information are also discussed.

Additional key words: apparent and functional PSII antenna size; driving forces; grouping (connectivity) probability; K-band; kinetics of P700 absorbance changes; K-step; L-band; OKJIP fluorescence rise kinetics.

Introduction

The decision of *Photosynthetica* to make a Special Issue on 'JIP-test in chlorophyll fluorescence and photosynthesis research' in Honour of Professor Reto J. Strasser must have been very welcomed by the photosynthesis research community, which highly respects his outstanding contribution to the field. The Special Issue comes 41 years after Strasser proposed his Theory of Energy Fluxes in Biomembranes (TEF) (Strasser 1978), 27 years after he published the OJIP polyphasic chlorophyll (Chl) *a* fluorescence rise kinetics obtained with a high time-resolution fluorimeter and plotted on logarithmic time-scale that reveals clearly the intermediate steps (Strasser and Govindjee 1992), and 24 years after he introduced the JIP-test (Strasser and Strasser 1995) by which OJIP is translated into biophysical parameters. All these years

Strasser has been also continuously teaching, not only through his publications, seminars, visits to many laboratories all over the world, but also with extensive answers and explanations to the many researchers asking his help.

Recognising these virtues, I considered as most pertinent to honour Professor Reto J. Strasser with an educative review revisiting the JIP-test. Having the privilege of a long collaboration with him, since 1994, essential components of which were our long, deep, and analytical discussions, even debates, which eventually led to improvements and necessary clarifications, the aim of this review was to (re)clarify concepts, assumptions, approximations, definitions and terminology of this powerful tool, as it was introduced and further developed by Strasser and his collaborators.

I deem that such (re)clarifications are indeed useful, as judged from problems and even flaws in comprehension

Received 16 August, accepted 12 November 2019.

Phone: 0035799456625, e-mail: tsimicha@spidernet.com.cy

Abbreviations: B_t – fraction of closed PSII RCs; Chl – chlorophyll; Cyt – cytochrome; F – fluorescence intensity emitted by PSII antenna (F_t : at time t); F_0 – minimal reliable recorded F (at O-step), taken commonly as the F emitted when all RCs are open; F_J and F_I – F at J- and I-step, respectively; F_P – maximal recorded F (at P-step); F_M – maximal F, when all RCs are closed; FNR – ferredoxin-NADP⁺-reductase; I_{act} – actinic light intensity; k_F – rate constant of PSII fluorescence emission; k_P and k_N – PSII photochemical and nonphotochemical deexcitation rate constants (k_N includes k_F); OEC – oxygen-evolving complex; OJIP – polyphasic Chl *a* fluorescence rise kinetics (O-step: at $t \cong 0$, J-step: at $t \cong 2$ ms, I-step: at $t \cong 30$ ms, P-step: peak of the rise kinetics); P680 and P700 – reaction centre pigments of PSII and PSI, respectively; PC – plastocyanin; p_G – grouping probability; Pheo – phaeophytin; PQ – plastoquinone; PQH₂ – plastoquinol; RC – reaction centre (here for PSII active reaction centres); RC^{si} – silent/inactive reaction centre (non-Q_A-reducing); TEF – Theory of Energy Fluxes in Biomembranes; ϕ_{P_0} – maximum quantum yield of PSII primary photochemistry. For further abbreviations used in the JIP-test, see Appendix.

and interpretation of obtained and obtainable parameters that appear in a non-negligible part of the huge and rapidly increasing literature applying the JIP-test and may further spread and increase confusion since it is not seldom that new papers refer to previous ones that carry such weaknesses.

Communication among scientists in any field demands the use of a uniform 'language'. The JIP-test, like any new approach or model, introduced several new parameters and defined necessarily terms and symbols for them; these need to be adopted by those who apply it, without inventing new ones. Parameters' definitions should be also used as introduced and improved. This is far from being considered as plagiarism to be avoided; it is a necessity for consistency, which also prevents erroneous rephrasing, indeed observed in several papers applying the JIP-test. Therefore, the present review can also be helpful in reminding and reestablishing the original terms, symbols, and definitions.

The JIP-test did not emerge out of 'parthenogenesis'; it was introduced and developed by Strasser as a continuation and advancement of his TEF, based on which he had already derived classic relations of biophysical parameters with fluorescence data obtainable before the polyphasic shape of OJIP was revealed (*see e.g.*, Strasser 1978, 1981). He then enriched the constellation of those parameters with parameters derived from the analysis of the richer in information OJIP to construct the JIP-test by a holistic approach. The present review will revisit the JIP-test in this order, starting from the (re)derivation of classic relations with the necessary clarifications, a part that can be of both interest and help also for readers who do not apply the JIP-test as a whole.

Modelling nature

What we know about any aspect in experimental sciences is the models we make for it. Construction and analysis of conceptual models are essential to address and understand the complexity of structure and function in nature. Models of any theoretical complexity can be formulated, but they are meaningful only if the experimental signals provide the resolution needed to validate them (Tsimilli-Michael and Strasser 2008a). Obviously this also holds true for the investigation of the photosynthetic machinery by means of Chl *a* fluorescence emitted by all photosynthetic organisms upon illumination. During the long history of these studies, the continuously developing theoretical/conceptual models used to interpret the obtained fluorescence signals, spectra and kinetics, have been subjected to criticism, which is the necessary motive force for advancement of both instrumentation/methods and the complexity of models. Despite their advancement, it cannot be claimed that the currently accepted models/concepts express 'the truth and nothing but the truth'. They still approximate events in nature and, when applying them, it is crucial to be aware of it. Unavoidably, the JIP-test is also based on assumptions and approximations, and the present article aims to contribute to their recognition and understanding.

The Kautsky fluorescence induction kinetics

There is a general agreement that Chl *a* fluorescence, emitted at room temperature by plants, algae, and cyanobacteria (though not true for all cyanobacteria) in the 680–740 nm spectral region, originates mainly from PSII and it can therefore serve as an intrinsic probe of the fate of its excitation energy (for reviews, *see* Papageorgiou and Govindjee 2004). Upon illumination, photosynthetic material exhibits a fluorescence induction kinetics, $F_t = f(t)$, first observed by Kautsky and Hirsch (1931), which shows an initial fast rise OP, from O (origin) to P (peak), whose duration (from less than 1 s up to several seconds) depends on the actinic light intensity, followed by a slower decrease PS (S for steady-state) lasting from seconds to minutes with several intermediate steps; hence, the P-step is a transitory steady-state (for an early review, *see* Govindjee 1995). Here, we will deal only with the rise kinetics to which the JIP-test routinely applies.

Information obtained from the fluorescence intensities at the extremes of the fluorescence rise kinetics

Even with experimental access only to the fluorescence intensities at O-step and P-step, their translation into biophysical parameters needs a theory/model, which, for all routine screenings (including the JIP-test) is the classic Duysens' concept (Duysens and Sweers 1963). According to this concept, the fluorescence emitted by a PSII unit upon illumination, which excites its antenna, is determined by the redox poise of its primary quinone electron acceptor Q_A : when Q_A is in the oxidised state, hence the reaction centre (RC) can perform photochemistry (open), F is low; when Q_A is in the reduced state (Q_A^-), hence the RC cannot perform photochemistry (closed), F is high. Concomitantly, the OP fluorescence rise reflects the accumulation of Q_A^- (of closed RCs), which is the net result of Q_A reduction due to PSII activity and Q_A^- reoxidation due to PSI activity. It is commonly accepted that, during the short time-interval of OP rise, no changes of the deexcitation rate constants of PSII antenna pigments and/or RC occur, while the subsequent PS-phase is determined both by Q_A^-/Q_A changes due to the competing PSII and PSI activities, and by conformational changes. An immediate consequence of Duysens' concept is that fluorescence intensity emitted by a sample being in any (but the same) conformation acquires its minimal value (F_0) when all RCs are open and its maximal value (F_M) when all RCs are closed. Though involvement of additional processes, which influence the fluorescence rise along with Q_A reduction, have been proposed (*see* Schansker *et al.* 2014 and references therein), Duysens' concept (called also 'the Q_A model') is widely accepted as a good approximation.

Note: The fluorescence signal recorded by any fluorimeter cannot be but intensity; actually, it is a fraction of the emitted intensity defined by a given for each fluorimeter geometrical factor and is therefore expressed in arbitrary intensity units (a.u.). The term 'fluorescence yield' used, instead, in several articles is basically wrong, unless it

means the unit-less ratio ‘fluorescence intensity/absorbed light intensity’ and not the signal as such.

It is obvious that, by their definition, both F_0 and F_M are biophysical parameters. Now comes the question how they are linked with the experimentally measured fluorescence intensities. It is not seldom that this apparently simple question is not addressed appropriately in routine applications, as it is taken blindly that F_P (at the P-step) corresponds to F_M and F at O-step to F_0 , misinterpreting subscript ‘0’ as standing for time zero (onset of illumination).

It needs to be emphasised that F_P is the fluorescence intensity emitted when the maximal possible, under the experimental conditions, fraction of RCs gets closed and it is equal to F_M only if the actinic light intensity, I_{act} , is strong enough to permit the complete closure of RCs and, even then, if all RCs can indeed get closed. The first aspect can be tested by using different I_{act} and select that one for which F_P/I_{act} gets saturated, provided that the light source can indeed supply it. The second aspect is less trivial, as there can be two main reasons that keep F_P lower than F_M . The one is the transformation upon stress of a fraction of RCs to non- Q_A -reducing centres (Strasser *et al.* 2004), which, however, can be detected and evaluated by the JIP-test (*see* subsection ‘Inactive/silent reaction centres’). The other is related to the status of ferredoxin-NADP⁺-reductase (FNR), which is inactive in darkness and needs light to get activated (Schansker *et al.* 2005). As elucidated in subsection ‘Information obtained from the JI- and IP-phases’, the complete closure of RCs is not achieved when FNR is active, unless much stronger actinic light could be used. It is worth bearing in mind this possibility, though the JIP-test applies for dark-adapted samples and the illumination duration to reach the P-step is not enough to activate FNR.

Note: Here, the cases of severe heat stress (*see* subsection ‘The K-step’), photoinhibition and/or UV stress, which strongly suppress F_P , are not considered, as the photosynthetic material is not anymore within physiological limits and none of the parameters derived by any method retains its biophysical meaning.

Concerning the fluorescence intensity at O-step, it is well-known that Q_A^- gets reoxidized in darkness (opening of RCs). Hence, the first question is whether the duration of darkness is enough to open all RCs, which needs to be tested by preliminary experiments; it should be taken into consideration that, in different plants, Q_A^- reoxidation in the dark may proceed with different rates and, moreover, stress may slow it down. The second question is whether the closed RCs can indeed open completely. If PQ (plastoquinone), which receives electrons from Q_A^- (and is in excess compared to total Q_A), gets or remains partially reduced (as PQH₂, plastoquinol) in the dark, a fraction of Q_A gets or remains reduced, due to an equilibration between Q_A^-/Q_A and PQH₂/PQ (*see* subsection ‘Information obtained from the OJ-phase’). This possibility can be checked by far-red preillumination so that PQH₂ gets reoxidised *via* PSI activity; the far-red intensity needs to be strong enough to oxidise PQH₂ without inducing PSII

activity. It is also possible that, under stress, a fraction of RCs remains closed in darkness, whatever its duration, even after far-red light exposure; though checking this possibility is difficult, it is worth keeping it in mind. The third question is whether the fluorimeter can indeed register the fluorescence intensity at ‘time zero’. When fluorimeters used shutters to turn-on illumination of the samples, this was solved by using low actinic light, which, however, had the disadvantage of leading to $F_P < F_M$. Nowadays, shutter-less fluorimeters with high time-resolution permit a quite precise detection of F at the onset of illumination, which can well be taken as the biophysical F_0 if all other prerequisites are fulfilled. For example, with the *Plant Efficiency Analysers (Hansatech Instruments Ltd., King's Lynn, Norfolk, UK)*, the first reliable measurement is at 50 μ s with the *PEA* fluorimeter, the oldest one, while in the newer (*HandyPEA, SeniorPEA, PocketPEA, M-PEA*) it is at 20 μ s; accordingly, $F_{50\mu s}$ and $F_{20\mu s}$ denote the experimental signals (*see* Appendix). For a higher precision, the first part of the transient (up to ~ 100 – 150 μ s) can be extrapolated down to time zero, assuming either an exponential shape of this part (Vredenberg 2000) or a linear one that fits quite well to the very initial part of both an exponential (non-connected PSII units) and a sigmoidal transient (connected PSII units) (Haldimann and Tsimilli-Michael 2005).

The maximum quantum yield of PSII primary photochemistry, ϕ_{P_0}

The basic biophysical parameter derived from the biophysical F_0 and F_M is the maximum quantum yield of PSII primary photochemistry, ϕ_{P_0} . The widely used formula inter-relating them was derived by expressing them in terms of the rate constants governing PSII antenna deexcitation; the photochemical (k_P) and the nonphotochemical (k_N), the latter including also k_F , the rate constant of PSII fluorescence emission (Kitajima and Butler 1975). By definition, only open RCs can perform photochemistry and, concomitantly, the according quantum yield is maximal when all RCs are open, given by:

$$\phi_{P_0} = k_P / (k_P + k_N) \quad (1)$$

With J_{abs} denoting the absorbed light intensity, F_0 and F_M are given as:

$$F_0 = J_{abs} \times k_F / (k_P + k_N) \quad (2)$$

$$F_M = J_{abs} \times k_F / k_N \quad (3)$$

Substitution of Eqs. 2 and 3 in Eq. 1 gives:

$$\phi_{P_0} = 1 - (F_0 / F_M) = (F_M - F_0) / F_M \quad (4)$$

Though models of higher complexity have been proposed, which formulate less simple equations, those given above are still widely used in all routine fluorescence analyses, and Eq. 4 is considered an accepted approximation for ϕ_{P_0} . Moreover, it is applicable independently of whether the PSII units are energetically connected or not, as neither F_0 nor F_M are affected by connectivity. In case

that it is not ensured that the experimental extremes correspond to the biophysical F_0 and F_M , the calculated $(F_M - F_0)/F_M$ expresses an ‘apparent’ ϕ_{P_0} .

Note: Though ‘yield’ implies transformation conserving energy, the complement of ϕ_{P_0} is called quantum yield of energy dissipation at time zero: $\phi_{D_0} = 1 - \phi_{P_0} = F_0/F_M$.

Solving Eqs. 2 and 3 for k_P and k_N gives:

$$k_P = J_{\text{abs}} \times k_F [(1/F_0) - (1/F_M)] \quad (5)$$

$$k_N = J_{\text{abs}} \times k_F \times (1/F_M) \quad (6)$$

If a stress is found to cause a decrease of F_M and a change of F_0 , and provided that it does not affect J_{abs} (k_F is anyway considered as constant), it can be deduced from Eqs. 5 and 6 whether the changes are due only to quenching at the antenna (increasing k_N but leaving k_P unaffected) or due to a change, also or exclusively, of k_P (effect on RC).

From Eqs. 2 and 3, the following is also derived:

$$k_P/k_N = (F_M - F_0)/F_0 \quad (7)$$

It should be noted that, since all expressions combining F_0 and F_M use in different combinations their ratio (hence J_{abs} cancels by division), they carry the same, and only one, piece of information. They only differ concerning the range of their values and, concomitantly, the extent of their dispersion (SD) in a set of replicates; *e.g.*, from ten replicates in a studied case, the following averages \pm SD were calculated: $(F_M - F_0)/F_M = 0.806 \pm 0.018$ (SD: 2.2%), $F_0/F_M = 0.194 \pm 0.018$ (SD: 9.2%), $F_M/F_0 = 5.2 \pm 0.5$ (SD: 10.3%), and $(F_M - F_0)/F_0 = 4.2 \pm 0.5$ (SD: 12.8%). In accordance with the above, care should also be taken when interpreting the impact of a stress on the different expressions; *e.g.*, in a studied case, $(F_M - F_0)/F_M$ decreased upon stress from 0.82 to 0.77 (6% decrease), F_0/F_M increased from 0.18 to 0.23 (28% increase), F_M/F_0 decreased from 5.56 to 4.35 (22% decrease), and $(F_M - F_0)/F_0$ decreased from 4.56 to 3.35 (27% decrease). Despite the wide differences in the sensitivities of these expressions, with ϕ_{P_0} being the most insensitive, all results quantify the same essential impact.

Information obtained from any F_t during fluorescence rise kinetics, in combination with F_0 and F_P (when $F_P = F_M$)

Variable, maximum variable and relative variable fluorescence

When the Kautsky kinetics was discovered, it was considered that the fluorescence rise kinetics was composed of a component that remained equal to F at the O-step – termed hence as ‘dead fluorescence’ – and an increasing component leading from O to P, hence termed as variable fluorescence. It was then proven that there is no ‘constant’ or ‘dead’ component and that the experimental F_t is simply the sum of the fluorescence emitted by all PSII antennae with open RCs (F_t^{op}) and all with closed RCs (F_t^{cl}). Still, the magnitude ‘variable fluorescence’, $F_v = (F_t - F_0)$, and the accordingly defined maximum variable fluorescence,

$F_v = (F_M - F_0)$, remain in use, employed also in the definition of the relative variable fluorescence, V_t ($0 \leq V_t \leq 1$):

$$V_t \equiv F_v/F_M = (F_t - F_0)/(F_M - F_0) \quad (8)$$

Contrary to F_v and F_M , V_t acquires also the property of a biophysical parameter, as it relates the biophysical parameters F_t^{cl} and F_t^{op} with F_M and F_0 , respectively:

$$V_t = F_t^{\text{cl}}/F_M \quad (9a)$$

$$V_t = (F_0 - F_t^{\text{op}})/F_0 \quad (9b)$$

Eqs. 9a and 9b give, respectively:

$$F_t^{\text{cl}} = F_M \times V_t \quad (10a)$$

$$F_t^{\text{op}} = F_0 \times (1 - V_t) \quad (10b)$$

Note: For the detailed derivations based on TEF equations in this and the next subsection, *see* Tsimilli-Michael and Strasser (2013a).

Addition of Eqs. 10a and 10b leads back to the experimental F_t :

$$F_t^{\text{op}} + F_t^{\text{cl}} = F_0 \times (1 - V_t) + F_M \times V_t = F_0 + (F_M - F_0) \times V_t = F_0 + F_v \times V_t = F_0 + F_v = F_t \quad (11)$$

What is very important in the above relations is that (1) they are valid independently of whether the PSII units are energetically separated or connected (grouped) and, (2) they permit the deconvolution of F_t kinetics into the fluorescence kinetics of open RCs and that of closed RCs.

Energetic connectivity is quantified by the grouping probability p_G ($= 0$ for separate units, $0 < p_G \leq 1$ for connected, $p_G = 1$ for the lake model). When p_G is different than zero, the excitation energy transferred between PSII units favours the units with open RCs, since the excitation energy in those with closed RCs is bigger than in those with open. Concomitantly, for any certain fraction of closed RCs, B , the excitation energy of the units with open RCs is bigger when $p_G \neq 0$ than when $p_G = 0$. This benefit is quantitatively demonstrated on the basis of the derived $V_t = f(B_i)$ equation, where B_i is the fraction of closed RCs:

$$V_t = \frac{B_i}{1 + [(F_v/F_0) \times p_G] \times (1 - B_i)} \quad (12)$$

Eq. 12 shows that $V_t < B_i$ for grouped units, while for separate units ($p_G = 0$) it degenerates to $V_t = B_i$. Applying each of the Eqs. 10a and 10b for $p_G = 0$ and $p_G \neq 0$, and using superscripts ‘un’ and ‘g’ for ‘ungrouped’ and ‘grouped’, respectively, gives:

$$F_t^{\text{cl,g}}/F_t^{\text{cl,un}} = V/B (= 1 \text{ for } p_G = 0; < 1 \text{ for } p_G \neq 0) \quad (13a)$$

$$F_t^{\text{op,g}}/F_t^{\text{op,un}} = (1 - V)/(1 - B) (= 1 \text{ for } p_G = 0; > 1 \text{ for } p_G \neq 0) \quad (13b)$$

It is worth noting that, as proven by Tsimilli-Michael and Strasser (2013a), even if a fraction of RCs becomes non- Q_A -reducing and, hence, the apparent F_M (F_M^{ap}) is lower than the true F_M , Eq. 12 still holds true, with F_v replaced by the apparent $F_v^{\text{ap}} = F_M^{\text{ap}} - F_0$.

Actual quantum yield of primary PSII photochemistry, ϕ_{Pt}

In accordance with Eq. 4, the actual quantum yield of primary PSII photochemistry, ϕ_{Pt} , at any time t during the fluorescence rise kinetics, is given by the well-known formula of Warren Butler (*see* Kitajima and Butler 1975):

$$\phi_{Pt} = 1 - (F_t/F_M) = (F_M - F_t)/F_M \quad (14)$$

Dividing Eq. 14 by Eq. 4, and recalling Eq. 8, we get:

$$\begin{aligned} \phi_{Pt}/\phi_{Po} &= (F_M - F_t)/(F_M - F_0) = 1 - [(F_t - F_0)/(F_M - F_0)] = \\ &= 1 - V_t \Leftrightarrow \phi_{Pt} = \phi_{Po} \times (1 - V_t) \end{aligned} \quad (15)$$

Eq. 15, as derived above, was reported by Paillotin (1976), while Strasser rederived it applying the TEF (*see* Strasser 1978, 1981). The Strasser's derivation can be summarised in a simple way as follows: primary PSII photochemistry is obviously performed only by the RCs that remain open and determined by the excitation energy of their antennae. So, ϕ_{Pt} , being proportional to the latter, is also proportional to F_t^{op} ; hence, and using Eq. 10b, we get:

$$\phi_{Pt}/\phi_{Po} = F_t^{op}/F_0 = (1 - V_t) \Leftrightarrow \phi_{Pt} = \phi_{Po} \times (1 - V_t) \quad (15')$$

The importance of Eq. 15' is that, due to Eq. 12, it is valid independently of the p_G value. Moreover, by comparison with $\phi_{Pt} = \phi_{Pt} \times (1 - B_t)$, to which it degenerates in the case of separate units, the essence of energetic connectivity for the 'economy' of photosynthesis is revealed: for the same B_t , $\phi_{Pt}^g = \phi_{Po} \times (1 - V_t) > \phi_{Pt}^{ng} = \phi_{Po} \times (1 - B_t)$, meaning that there is gain in ϕ_{Pt} when the units are connected.

The polyphasic OJIP fluorescence transient

Already 52 years ago, it was recognized that the O-P fluorescence rise is not monophasic (Delosme 1967). Several reports since then showed one or two intermediate step(s) between O and P (*see e.g.*, Neubauer and Schreiber 1987). However, the detailed shape of the polyphasic fluorescence transient was revealed (Strasser and Govindjee 1992, Strasser *et al.* 1995) only when the fluorescence signals, induced by strong illumination and recorded with a high time-resolution instrument over a wide time range, were plotted on a logarithmic time scale; the instrument used at that time was the *PEA* fluorimeter, with data acquisition every 10 μ s for the first 2 ms and every 1 ms thereafter. (*Note:* With *HandyPEA*, *SeniorPEA*, *PocketPEA*, and *M-PEA*, the data acquisition is every 10 μ s for the first 0.3 ms, every 0.1 ms until 3 ms, every 1 ms until 30 ms, and so on).

Under continuous red actinic light (peak at 650 nm) of 3,000 μ mol(photon) $m^{-2} s^{-1}$, the fluorescence transient exhibits the steps J (F_J , at 2 ms) and I (F_I , at 30 ms) between the initial O (F_0) and the maximum P (F_P), hence labelled as OJIP (main plot of Fig. 1). Based on this notation, the test that translates extracted data from OJIP into biophysical parameters was termed as 'JIP-test'. (*Note:* the correct nomenclature denotes J and I as 'steps', and OJ, JI, and IP as 'phases').

Fig. 1 depicts transients exhibited by the same material (here pea leaves) upon actinic illumination of different

intensities, I_{act} , given as percentages (100, 75, 50, and 25%) of the 3,000 μ mol(photon) $m^{-2} s^{-1}$, the maximum applied I_{act} ; to facilitate comparison, the obtained transients were multiplied by 1, 4/3, 2, and 4, respectively. As shown, the 100% intensity is more than enough to close all RCs (provided that complete closure is permitted), and F_P is hence equal to F_M ; even when I_{act} is 25%, F_P almost reaches F_M . On the other hand, F_J and F_I get lower by lowering I_{act} , while at 25% the J-step vanishes as step. Hence, though nothing forbids the use of any I_{act} for the induction of fluorescence kinetics, when the JIP-test is to be applied, care should be taken to use such an I_{act} that F_M is reached and the J- and I-steps are clearly revealed; the 3,000 μ mol(photon) $m^{-2} s^{-1}$ is a safe choice, as judged from studies on leaves from a variety of plants.

Fluorescence kinetics are the real thing, independent of the model used

Nature's structure and function do not depend on concepts and methods. The same is true for the fluorescence transient. This simple statement is here emphasised, because the ease and quickness of applying OJIP analysis

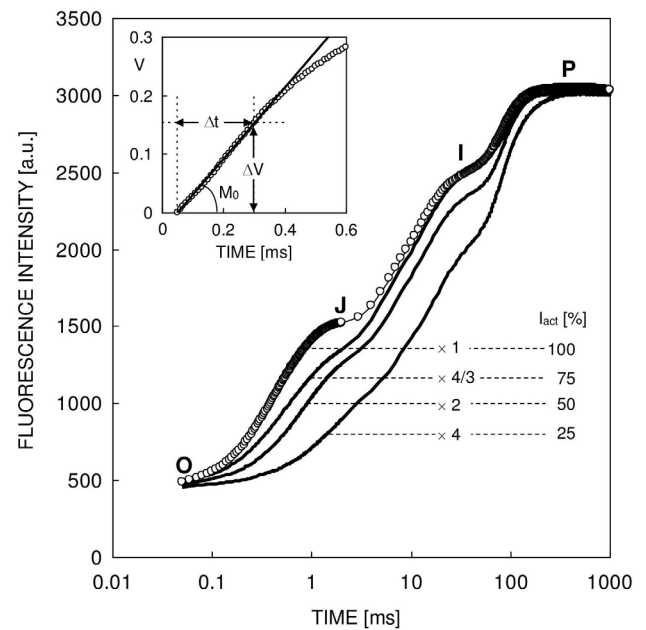


Fig. 1. A typical Chl *a* fluorescence rise kinetics OJIP (*open circles*), exhibited upon illumination of a dark-adapted photosynthetic sample (here a pea leaf) by strong red light [3,000 μ mol(photon) $m^{-2} s^{-1}$; peak at 650 nm] and measured with the *PEA*-fluorimeter, plotted on a logarithmic time scale; the steps O (at 50 μ s), J (at 2 ms), I (at 30 ms), and P (peak) are marked. Transients obtained with lower actinic light intensities, I_{act} (indicated as percentages of the highest intensity used) are also depicted (*lines*, no markers). In order to facilitate comparison, the obtained data with I_{act} : 100, 75, 50, and 25% were multiplied by 1, 4/3, 2, and 4, respectively. The insert depicts the transient obtained with the maximal I_{act} , expressed as relative variable fluorescence $V_t = (F_t - F_0)/(F_M - F_0) = f(t)$, plotted on a linear time scale from 50 μ s to 0.6 ms, demonstrating how the initial slope is calculated: $M_0 = (\Delta V/\Delta t)_0 = (V_{300\mu s})/(0.25 \text{ ms})$.

by the JIP-test with a readymade software have been so tempting in conducting routine investigations that it is not seldom that publications depict, even in multiple graphs, the end results of JIP-test analysis, mostly as averages of the calculated parameters, while they show, if at all, average transients and, even then, only after normalization.

Raw vs. average fluorescence transients

The raw fluorescence transient $F_t = f(t)$ is the real thing and, before applying any calculation, it is unequivocal that all raw transients in an obtained set of replicates should be plotted to be examined. The first and simple reason is to examine whether any of them have unusual or unexpected or even distorted shape, which would indicate a problem in handling the samples or a technical measuring problem to be solved. The second reason is to visualise and recognise their dispersion, which can provide an important piece of information on natural heterogeneity and evaluation of its extent, as shown in Fig. 2. (see also Tsimilli-Michael and Strasser 2013b).

Raw vs. normalised fluorescence transients

Two main normalizations are commonly used to depict the fluorescence transients: (1) Normalization on F_0 , i.e., plotting $F_t/F_0 = f(t)$. Provided that all prerequisites permitting the detection of the biophysical F_0 are fulfilled, this normalization is not only permitted, but necessary to overcome heterogeneity with respect to the absorbance of the excited cross section of the samples; even then, it needs to be commented whether observed variations of F_0 values are random and with which dispersion, or follow a trend under the given treatment. (2) Calculation and plotting of $V_t = f(t)$. The information from such a plot can be distorted either because the recorded initial fluorescence is not the biophysical F_0 and/or because $F_p < F_M$. An example demonstrating the above discussed pros and cons is shown in Fig. 3, where normalization on F at O-step is well permitted, while plotting of $V_t = f(t)$ obscures

almost completely the stress effect. On the other hand, in Fig. 4 depicting cases, where F at O-step is far from being equal to the real F_0 (see subsection ‘Information obtained from the OJ-phase’), it is more than obvious that a ‘blind’ normalization on it would give completely wrong information.

The JIP-test: translation of experimental signals into biophysical parameters

Measurement of fluorescence kinetics aims to provide an insight into the structure and function of the photosynthetic apparatus. In order to make the link between the measured fluorescence intensities and parameters quantifying structure and function, we need a theory and a model; this holds true for any experimental signal that needs to be translated into biophysical parameters.

Since any model is an approximation of reality and can be questioned in the future (or even in the present), it is important to make the distinction between experimental data extracted from the OJIP, basic parameters calculated from the extracted data independently of the JIP-test model and biophysical parameters derived from the basic parameters by the JIP-test model. In this way, communication among researchers is facilitated and the huge amount of experimental data can be processed by other current models, as well by models that will be developed in the future. Appendix presents, following this classification, all the parameters used by the JIP-test that are discussed below, as well as those already discussed above.

Energy fluxes and yields/probabilities/efficiencies as flux ratios

Basics from the Theory of Energy Fluxes (TEF)

There is no energy transforming system that fully conserves energy when transforming one form (energy input) into another (energy output), due to energy losses as heat. In other words, the efficiency of any transformer,

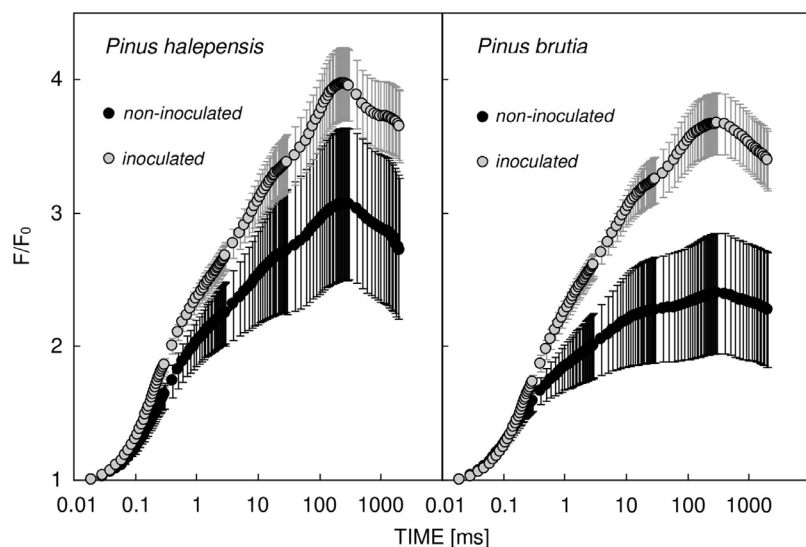


Fig. 2. Average \pm SD ($n = 50$) fluorescence transients OJIP of dark-adapted needles of *Pinus halepensis* (left panel) and *Pinus brutia* (right panel) trees grown in a gypsum quarry (in Cyprus), without (black circles) or with inoculation with a commercial mixture of ectomycorrhiza (gray circles), plotted on logarithmic time scale as $F_t/F_0 = f(t)$; the transients were induced by strong red light [$3,000 \mu\text{mol}(\text{photon}) \text{m}^{-2} \text{s}^{-1}$; peak at 650 nm] and measured with *Handy PEA*. (Raw data were obtained from Tsimilli-Michael *et al.* 2008).

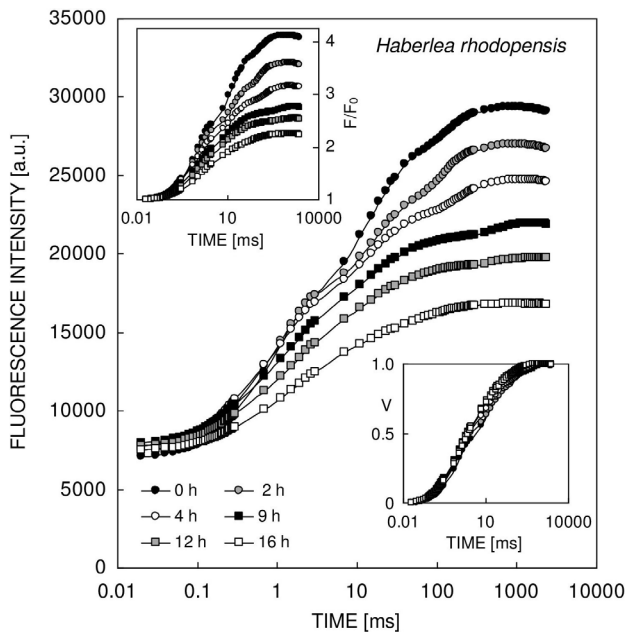


Fig. 3. Main plot: OJIP fluorescence transients, $F_t = f(t)$, induced by strong red actinic light [$5,000 \mu\text{mol}(\text{photon}) \text{m}^{-2} \text{s}^{-1}$; peak at 627 nm] and measured with *M-PEA* on dark-adapted intact leaves of *Haberlea rhodopensis* attached to the plants that were subjected to gradual water loss in darkness (drying time is indicated). *Upper* and *lower inserts* depict, respectively, the same transients expressed as $F_t/F_0 = f(t)$ and $V_t = f(t)$. (Raw data were obtained from Strasser *et al.* 2010).

i.e., the ratio (energy output)/(energy input), which can be equivalently called as yield, is smaller than unity. Taking into consideration that in nature a continuum of energy supply exists, the TEF considers fluxes of energy (energy/time): energy influxes (E_{influx}) and energy outfluxes (E_{outflux}) (Strasser 1978, 1981; also see Tsimilli-Michael and Strasser 2013a). Accordingly, the efficiency or yield is defined as the flux ratio $E_{\text{outflux}}/E_{\text{influx}}$. All these terms are also equivalent to the probability that E_{influx} is transformed into E_{outflux} ; this equivalency is important because probabilities are related to rate constants.

Any process with sequential transformations of energy fluxes can be considered as operated by a macro-transformer, consisting of a series of individual micro-transformers, each of which is characterised by a yield/efficiency or, equivalently, by the probability to conserve energy. Hence, we deal with several yields/efficiencies/probabilities. Moreover, any sequential sub-assembly of these individual micro-transformers can be considered as a semi-micro-transformer. This permits us to ‘break’, in an investigation, the macro- to those semi-micro- that can be assessed by the applied experimental procedure, if assessment of each of the micro-components is not possible or, even, if not all of them have been identified.

Such a series is schematically shown in Fig. 5, where the energy fluxes (E_i ; $i = 1, 2, \dots, n$) are presented by arrows and the transformers by boxes, in each of which the probability ($p_{ij} = E_j/E_i$; $i = 1, \dots, n - 1$; $j = i + 1$) for the transformation they perform is indicated. The

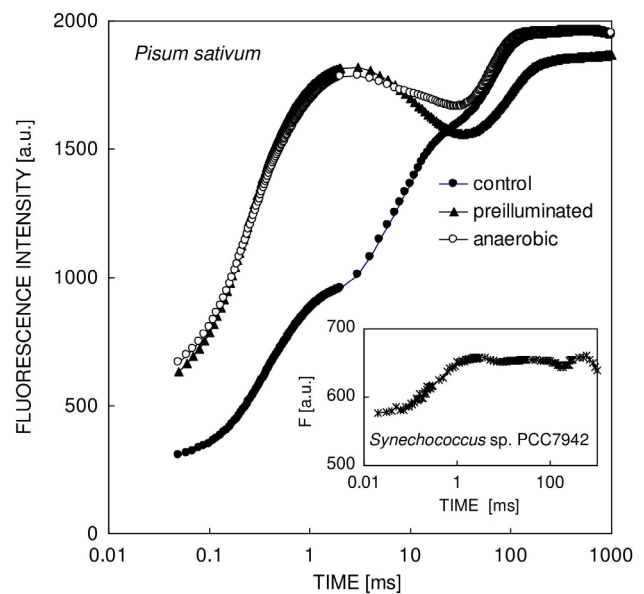


Fig. 4. Main plot: Chl *a* fluorescence transients $F_t = f(t)$ exhibited by leaves of pea plant (*Pisum sativum*) under the following conditions: dark-adapted (control; *closed circles*), preilluminated for 1 s (with the same light used to induce the transients) followed by 10-s darkness (*closed triangles*), and dark-adapted under anaerobic conditions (flushing with N_2) (*open circles*). For other details, see legend of Fig. 1. Raw data were provided by Pierre Haldimann (from Haldimann and Strasser 1999). *Insert*: The fluorescence transient exhibited by dark-adapted *Synechococcus* sp. PCC7942 cells and measured with *Handy PEA* (see legend of Fig. 2); note that the scale of the vertical axis starts at 500. (Raw data were obtained from Tsimilli-Michael *et al.* 2009).

scheme depicts also the relation between the probability (efficiency), p_{1n} , of the macro-transformer (from E_1 to E_n), and that of a selected (as example) semi-micro-transformer, p_{13} (E_1 to E_3), with the probabilities/efficiencies of the individual micro-transformers.

Further than the terms referred above, which hold for any transformation, the term quantum yield (ϕ) is exclusively used for the transformations of the absorbed light energy influx (quanta/time).

Applying the basics of the TEF in the JIP-test

The approach summarised above was the basis for the proposition and the development of the JIP-test, with the photosynthetic electron transport chain from the primary photochemical reduction of Q_A by PSII until the reduction of electron acceptors after PSI considered as the macro-transformer.

The Q_A redox poise, accepted to be reflected in the fluorescence rise kinetics, is governed by the redox poises of the carriers in the electron transport chain, which are controlled by PSII photoreducing activity and the competing PSI photochemical activity that reoxidises the intersystem chain and reduces PSI electron acceptors. The rates of the successive oxidoreduction reactions are governed by the size and poise of the carriers' pools and

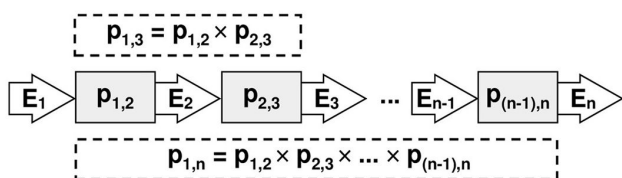


Fig. 5. A schematic presentation of sequential transformations of energy fluxes by a series of micro-transformers; energy losses are not indicated. The energy fluxes (E_i ; $i = 1, 2, \dots, n$) are presented by wide arrows and the micro-transformers by boxes, in each of which the probability ($p_{i,j} = E_j/E_i$; $i = 1, \dots, n-1$; $j = i+1$) for the transformation they perform is indicated. *Dashed-line boxes* correspond to the macro-transformer of E_1 to E_n and to a selected, as example, semi-micro-transformer of E_1 to E_3 , with their transformation probabilities, $p_{1,n}$ and $p_{1,3}$ respectively, given as products of the probabilities of their micro-transformers' components.

the respective rate constants. Each carrier can hence be considered as a micro-transformer with its own efficiency.

Although OJIP transient and the JIP-test do not provide access to each of the micro-transformers, they do provide access to semi-micro-transformers utilising the appearance of the distinct intermediate steps J and I. These steps reflect transitory steady-states of Q_A^- concentration, as at the time instants they appear, the slope of the fluorescence kinetics (dF_J/dt and dF_I/dt) is equal (or can well be approximated as equal) to zero, meaning that at each of them, the rate of Q_A reduction is equal to the rate of Q_A^- reoxidation. They hence reveal sequential kinetic bottlenecks in the electron flux, which permit the distinction between three successive semi-micro-transformers, with the energy fluxes they transform defined as: ABS – the absorption flux (photons flux absorbed by PSII antenna) creating excited Chl *a* (Chl*); TR – the trapping flux channelled to the reaction centre to be converted to redox energy reducing phaeophytin (Pheo) and Q_A (to Q_A^-); ET – the electron transport flux from Q_A^- (which is hence reoxidised to Q_A) to the intersystem electron carriers, *i.e.*, Q_B , PQ – cytochrome (Cyt) *b₆/f* and PC (plastocyanin); RE – the electron flux from PQH₂ that, driven by PSI, reduces PSI end electron acceptors.

The energy fluxes expressed per RC (PSII active/ Q_A -reducing reaction centre) are defined by the JIP-test as specific energy fluxes; their values, as determined (*see below*), are in ms^{-1} and on an arbitrary scale, common however for all. The JIP-test defines also the respective quantum yields (q.y.), as the ratios of the fluxes per ABS: $\varphi_P \equiv TR/ABS$, the q.y. of primary photochemistry; $\varphi_E \equiv ET/ABS$, the q.y. of electron flux beyond Q_A^- ; $\varphi_R \equiv RE/ABS$, the q.y. of electron flux to PSI end electron acceptors. As flux ratios, quantum yields are unitless and on absolute scale, since the arbitrariness of the fluxes' scale cancels by division. (For definitions, *see Fig. 6 and Appendix*).

Note: In older publications of Strasser and collaborators (*see e.g.*, Strasser *et al.* 2004), the energy fluxes per excited cross section (CS), termed as phenomenological fluxes, were also calculated by multiplying the quantum yields by ABS/CS, which was approximated by F_0 – assumed to have

a constant yield throughout an experiment – and was hence denoted as ABS/CS₀. This approximation has been mostly abandoned by Strasser and collaborators, as it was rather unsafe. With the *Multifunctional Plant Efficiency Analyser M-PEA* (for a description, *see Strasser et al.* 2010), as well as with other instruments, the relative absorptivity of the leaf is measured, hence ABS/CS is directly obtained and the phenomenological fluxes can be determined, if needed.

Let us now see how the JIP-test, analysing the OJIP, provides information about the specific fluxes, the quantum yields, and the other efficiencies in the energy cascade.

Information obtained from the OJ-phase

Specific energy fluxes, quantum yields and other efficiencies

At any time t , TR_t/RC expresses the rate (in ms^{-1}) by which excitons are trapped by RCs resulting in the reduction of Q_A to Q_A^- . In order to get an experimental access to the determination of this rate, the reasoning of the JIP-test started from the case of DCMU-poisoned samples: since Q_A^- reoxidation is inhibited ($ET = 0$), trapping leads, without competing oxidation reactions, to the complete closure of all RCs. Hence, TR_t/RC is equal to $(dB/dt)_t$, which, in turn, is related to $(dV/dt)_t$ by the following equation [deduced after expressing Eq. 12 as $B = f(V)$], where $C_{HYP} = p_G \times (F_V/F_0)$:

$$\frac{TR_t}{RC} = \left[\frac{dB}{dt} \right]_{t,DCMU} = \frac{(1 + C_{HYP})}{(1 + C_{HYP} \times V_t)^2} \left[\frac{dV}{dt} \right]_{t,DCMU} \quad (16)$$

When $p_G = 0$ (separate units), Eq. 16 degenerates to:

$$TR_t/RC = (dB/dt)_{t,DCMU} = (dV/dt)_{t,DCMU} \quad (16')$$

For a thorough analysis of energetic connectivity, including the derivation of Eqs. 16 and 16', the reader can consult Strasser *et al.* (2004) and Tsimilli-Michael and Strasser (2013a). Two basic aspects, for the case of DCMU-poisoned samples, need to be recalled here: (1) $V_t = f(B_t)$ is a hyperbolic function, as expressed by Eq. 12; the parameter C_{HYP} stands for the curvature of the hyperbola. (2) The fluorescence rise kinetics is sigmoidal and not exponential as it would be for the case of separate units ($p_G = 0$) for which Q_A reduction would be a first order reaction.

The maximal value of TR_t/RC is at $t = 0$ (denoted as TR_0/RC), since all RCs are then open ($B = 0$, $V = 0$). From Eq. 16 we get:

$$TR_0/RC = (dB/dt)_{0,DCMU} = (1 + C_{HYP}) \times (dV/dt)_{0,DCMU} \quad (17)$$

Therefore, in order to calculate TR_0/RC from the initial slope $(dV/dt)_{0,DCMU}$, we need to know C_{HYP} . Though Strasser (1978, 1981) did propose a way to calculate it (for a review, *see Strasser et al.* 2004), for a routine test a simpler approach was later adopted, based on the finding that, under the actinic light used for the JIP-test, all sigmoidal fluorescence induction curves, independently of their C_{HYP} value, cross the exponential curve ($C_{HYP} = 0$) at

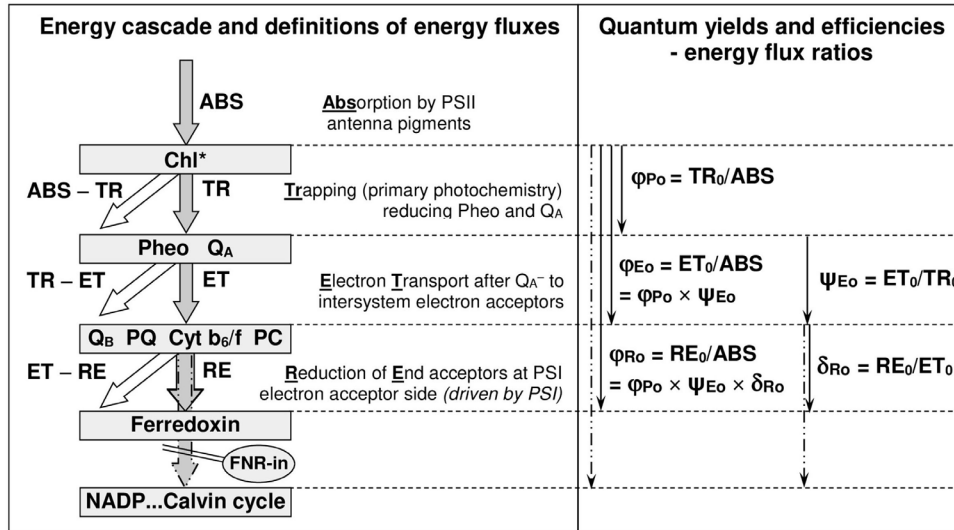


Fig. 6. The sequential transformations of energy fluxes (*wide gray arrows*) from ABS (absorption by PSII antenna), to TR (reducing Pheo and Q_A), to ET (reducing the intersystem electron acceptors Q_B, PQ, Cyt b₆/f, PC), up to RE (reducing PSI end electron acceptors); the outfluxes dissipating energy are indicated by *wide white arrows*. PSI electron acceptors include only those up to ferredoxin if FNR is inactive, or all up to the Calvin-Benson cycle and CO₂ fixation if FNR is active. The quantum yields and the other efficiencies for energy conservation, as flux ratios, are also defined, indicated by *thin line arrows*; for the case of active FNR *dash-dotted lines* are used instead. (Modified from Tsimilli-Michael and Strasser 2008b).

300 μs (Strasser and Strasser 1995). Hence, for both the cases of grouped and separate units, an approximation of (dV/dt)_{0,DCMU} as (ΔV/Δt)_{0,DCMU} between 50 and 300 μs was taken as the initial slope, denoted as M_{0,DCMU} (in ms⁻¹; note that Δt is expressed in ms):

$$\begin{aligned} TR_0/RC &= M_{0,DCMU} \cong (\Delta V/\Delta t)_{0,DCMU} = \\ &= [(F_{300\mu s} - F_{50\mu s})/(F_M - F_0)]_{DCMU}/(0.30 - 0.05) = \\ &= 4 \times [(F_{300\mu s} - F_{50\mu s})/(F_M - F_0)]_{DCMU} \quad (18) \end{aligned}$$

Note: The JIP-test was introduced when OJIP was recorded with the *PEA* fluorimeter, with which the first reliable point was at 50 μs. Though with new instruments (*HandyPEA*, *SeniorPEA*, *PocketPEA* and *M-PEA*), the first reliable value is F_{20μs} (hence used as the F₀), Eq. 18 has remained in use, as introduced.

Obviously, Eq. 18 is not valid when Q_A⁻ reoxidation is not blocked; hence, the observed initial slope, denoted now as M₀ and given as M₀ ≅ (ΔV/Δt)₀ = 4 × (V_{300μs} - V_{50μs}) (see also insert of Fig. 1), expresses the net rate of the RCs' closure with TR₀/RC increasing the number of closed RCs and ET₀/RC decreasing it:

$$M_0 = (\Delta V_t/\Delta t)_0 = TR_0/RC - ET_0/RC \quad (19)$$

It was observed that, under the same actinic illumination, 3,000 μmol(photon) m⁻² s⁻¹, the J-step appears at (about) the same time (2 ms) as the maximum fluorescence in DCMU-poisoned samples. This led to an investigation that compared the OJ-phase, normalized between O and J, *i.e.*, expressed as W_{(OJ),t} ≅ (F_t - F₀)/(F_J - F₀) = V_t/V_J = f(t), with the V_t = f(t) of DCMU-treated samples. A good coincidence between the two curves was found (Strasser and Strasser 1995), also with respect to their sigmoidicity. Sigmoidal and exponential W_{(OJ),t} = f(t) cross at 300 μs,

as for the case of V_t = f(t) in DCMU-inhibited samples (see *e.g.*, Strasser and Stirbet 2001).

Note: W_{(OJ),t} appears commonly in the literature as W_t, as it was originally denoted (Strasser *et al.* 2004). However, since other similar types of normalization were later introduced (Strasser *et al.* 2007), the notations need to be written as W_{(YZ),t}, where Y and Z refer to the beginning and end point of the normalization, and defined as W_{(YZ),t} ≅ (F_t - F_Y)/(F_Z - F_Y). (See Appendix and subsection 'Semi-quantitative information from OJIP normalizations').

Based on the good coincidence between W_{(OJ),t} = f(t) and V_{t,DCMU} = f(t), M_{0,DCMU} was simulated by the multiplication of M₀ by 1/V_J, equivalently by the initial slope of W_{(OJ),t}; concomitantly,

$$TR_0/RC = M_{0,DCMU} = M_0/V_J = (\Delta W_{(OJ),t}/\Delta t)_0 \quad (20)$$

Combination of Eqs. 19 and 20 gives:

$$\begin{aligned} ET_0/RC &= TR_0/RC - M_0 = (TR_0/RC) - [(TR_0/RC) \times V_J] = \\ &= (TR_0/RC) \times (1 - V_J) = (M_0/V_J) \times (1 - V_J) \quad (21) \end{aligned}$$

Hence, the probability ψ_{E₀} that a trapped exciton moves an electron into the electron transport chain beyond Q_A⁻, is given as:

$$\psi_{E_0} \equiv ET_0/TR_0 = (ET_0/RC)/(TR_0/RC) = 1 - V_J \quad (22)$$

Using the definition φ_{P₀} ≅ TR₀/ABS, Eq. 4 is written as:

$$\phi_{P_0} \equiv TR_0/ABS = 1 - (F_0/F_M) \quad (23)$$

Hence, φ_{E₀} is derived as:

$$\begin{aligned} \phi_{E_0} \equiv ET_0/ABS &= (TR_0/ABS) \times (ET_0/TR_0) = \phi_{P_0} \times \psi_{E_0} = \\ &= [1 - (F_0/F_M)] \times (1 - V_J) \quad (24) \end{aligned}$$

The above equation may also be deduced as follows: the

J-step reflects a transitory steady-state of Q_A^- concentration ($dF_J/dt \cong 0$), meaning that the rate of Q_A reduction is equal to the rate of Q_A^- reoxidation; hence $\phi_{E_0} = \phi_{P_j}$. Recalling also the general Eq. 15 for ϕ_{pt} and applying it for the J-step (ϕ_{P_j}), we get:

$$\phi_{E_0} = \phi_{P_j} = \phi_{P_0} \times (1 - V_j) \quad (24')$$

The reasoning presented above implies that the OJ-phase reflects photochemical reduction of Q_A and partial reoxidation of Q_A^- by PQ (via Q_B); accordingly, the bottleneck at J-step was attributed to a limitation in the exchange of a PQH_2 molecule at the Q_B site with an oxidised PQ molecule (see e.g., Schansker *et al.* 2005). This attribution was also supported by studies revealing an increased V_j (concomitantly, a decreased ψ_{E_0}) when the PQ pool is partially reduced prior to fluorescence measurements, as happens under anaerobic conditions (see e.g., Haldimann and Strasser 1999, Haldimann and Tsimilli-Michael 2005) or after a preillumination followed by a short dark interval (see e.g., Schansker *et al.* 2005), as well as in cyanobacteria due to the respiration-driven accumulation of PQH_2 in the dark since respiratory and photosynthetic electron flow share the same PQ pool (for *Synechococcus* sp. PCC7942, see Tsimilli-Michael *et al.* 2009). Examples are presented in Fig. 4, which also demonstrate the effect on F at O-step, due to an equilibration between Q_A^-/Q_A and PQH_2/PQ .

From Eqs. 20 and 23, the specific absorption flux ABS/RC is derived as:

$$\begin{aligned} \text{ABS/RC} &= (\text{TR}_0/\text{RC})/(\text{TR}_0/\text{ABS}) = (\text{TR}_0/\text{RC})/\phi_{P_0} = \\ &= (M_0/V_j)/[1 - (F_0/F_M)] \end{aligned} \quad (25)$$

The specific energy flux for dissipation is also calculated, as $DI_0/\text{RC} = \text{ABS/RC} - \text{TR}_0/\text{RC}$. (For the definitions, see Fig. 6 and Appendix).

Inactive/silent reaction centres

The present review has already referred to Q_A -reducing and non- Q_A -reducing reaction centres, denoted as active and inactive (or silent, RC^{si}), respectively, clarifying also that the notation 'RC' is used only for the former. Inactivation of a fraction of RCs was proposed to explain the findings that, upon several types of stress, OJIP, though induced by saturating I_{act} , exhibits a lower F_M , while F_0 and TR_0/RC remain unaffected (Krüger *et al.* 1997, Strasser and Tsimilli-Michael 1998). The combination of decreased F_M and stable F_0 excludes the possibility of quenching at the antenna (see comments on Eqs. 5 and 6). On the other hand, the stability of TR_0/RC means stability of trapping by those reaction centres (RCs) that can reduce Q_A (since TR_0/RC is calculated from the V_t kinetics). In our proposition, inactive/silent centres dissipate the entire energy outflux that they would use for photochemistry if they were active; they hence behave throughout the fluorescence induction as open RCs with respect to the fluorescence they emit, which is in agreement with the stability of F_0 (see Strasser *et al.* 2004 and references therein, Tsimilli-Michael and Strasser 2013a).

When a fraction of RCs is transformed to RC^{si} , the experimental ratio F_v/F_M , which should more correctly be then written as $F_v^{ap}/F_M^{ap} = 1 - F_0/F_M^{ap}$, expresses the apparent ϕ_{P_0} ($\phi_{P_0}^{ap}$) of the mixture of PSII units with RC (performing photochemistry) and units with RC^{si} (zero photochemistry); the same applies for the k_p . Recalling the definition of ϕ_{P_0} as TR_0/ABS , it would now read as TR_0 (anyway, only by active) divided by the absorption flux by all PSII units, both with RC and RC^{si} , in the excited cross section.

Accordingly, ABS/RC , calculated from Eq. 25, is proportional to the total amount of absorbing chlorophylls per RC, meaning that it provides, on a relative scale, a measure of the apparent antenna size, which is unitless (though ABS/RC as energy flux is in ms^{-1}). Concomitantly, the reciprocal of ABS/RC expresses the molar ratio (on a relative scale) of RCs to the absorbing chlorophylls:

$$\text{RC/ABS} = (\text{TR}_0/\text{ABS})/(\text{TR}_0/\text{RC}) \quad (26)$$

The fraction of RCs that remain active after a stress, denoted as 'x', and the fraction (1 - x) of those inactivated as RC^{si} are calculated applying Eq. 26 for nonstressed (control; subscript 'c') and stressed samples:

$$\begin{aligned} x &= [\text{RC}/(\text{RC})_c] = [\text{RC/ABS}]/[(\text{RC})_c/\text{ABS}] \Leftrightarrow \\ 1 - x &= 1 - [\text{RC/ABS}]/[(\text{RC})_c/\text{ABS}] \end{aligned} \quad (27)$$

Apparent and functional antenna size

Although inactivation of RCs was proposed to explain how TR_0/RC could remain unaltered upon a stress while TR_0/ABS (as F_v/F_M) decreased, Eq. 26 is also valid when both undergo changes (since RC/ABS is calculated from both). In case that TR_0/RC increases while TR_0/ABS undergoes smaller changes and, thus, the increase of ABS/RC follows basically that of TR_0/RC (see Eq. 25), it means that we are witnessing an increase of functional antenna size, *i.e.*, of the antenna that does supply excitation energy to active RCs. In cases that both TR_0/RC and TR_0/ABS are affected, Eqs. 25–27 can reveal that both apparent and functional antenna size, or none of them, have undergone changes.

The grouping probability p_G

As already recalled, $W_{(O),t} = f(t)$ is exponential in the case of separate units and sigmoidal, with different degrees of sigmoidicity, in the case of energetically connected (grouped) units, with the kinetics crossing at 300 μs . In order to calculate the grouping probability p_G , the case of $p_G = 0$ was simulated by an exponential curve that keeps all the other features of the sample under study, denoted (subscript 'E' for exponential) as $W_{E(O),t} = f(t)$. The difference $W_{E(O),t} - W_{(O),t}$ of the (any) actual sigmoidal from the simulated exponential curve depends obviously on the extent of grouping; the overall grouping probability p_G is calculated by the following formula that utilizes the maximal difference, appearing at 100 μs (Stirbet *et al.* 1998, Strasser and Stirbet 2001):

$$P_G = \frac{(W_{E(OJ),100\mu s} - W_{(OJ),100\mu s})}{W_{(OJ),100\mu s} \times (1 - W_{E(OJ),300\mu s} \times V_J) \times V_J} \times \frac{F_0}{(F_M - F_0)} \quad (28)$$

where $W_{E(OJ),100\mu s} = 1 - (1 - W_{(OJ),300\mu s})^{1/5}$

The K-step

Under various stress conditions, such as heat or drought stress, an early step (as a shoulder or, even a local peak under severe stress) was found to appear at about 300 μ s in the fluorescence rise kinetics (Guissé *et al.* 1995); the step was labelled as K-step and, accordingly, the transient exhibiting it as OKJIP. Under severe stress, the K-step becomes predominant and the P-level is highly suppressed. The OKJIP transient was also found to be exhibited by different higher plants growing naturally in ecosystems with dry and hot environment (Srivastava *et al.* 1997). A number of investigations by Strasser and collaborators have provided evidence that the K-step is related to the inactivation of the oxygen-evolving complex (OEC) and the concomitant reduction of P680⁺ (P680: PSII RC) and Q_A by other endogenous electron pools; this flow, ‘bypassing’ the physiological rate-limiting reactions that are at OEC (Lazár *et al.* 1997), proceeds with a higher rate, thus resulting in the early appearing K-step. As the endogenous pools are not regenerated, they are quickly exhausted and, concomitantly, fluorescence intensity never reaches the F_M level (*see* Strasser *et al.* 2004 and references therein). *Note:* Care should be taken to avoid using the notation F_K as interchangeable with the notation F_{300 μ s}: though they both refer to 300 μ s, F_K implies that K-step does exist (OKJIP transient), while F_{300 μ s} is one of the extracted values from OJIP.

Information obtained from the JI- and IP-phases

Interpretation of the JI- and IP-phases further supported by simultaneous recording of the modulated reflection at 820 nm

The OJIP fluorescence rise reflects Q_A reduction, with Q_A poise depending on the poise of the intersystem electron carriers, which, in turn, depends also on the redox state of P700 (PSI reaction centre). There is strong evidence that the JI-phase reflects (mainly) the reduction of the intersystem electron carriers Q_B, PQ, and Cyt *b₆f*, defined by their size (mainly of PQ) and the rate constants of the reactions that follow, while the IP-phase reflects the reduction, with electrons delivered by PQH₂, of PC⁺, P700⁺, and of PSI end electron acceptors (RE), driven by PSI activity.

The first to clarify is that the term ‘PSI electron acceptors’ means those acceptors that can function as such until fluorescence transient reaches its peak (F_P). The size of their pool depends on the status of FNR: in darkness, FNR is inactive and its activation is not realised within the less than 1-s illumination needed to reach F_P. Thus, in dark-adapted samples, the above term includes only the

PSI electron acceptors until FNR, while an active FNR permits electron flow to a much bigger pool of electron acceptors after PSI, up to the Calvin-Benson cycle; this is schematically shown in Fig. 6. When FNR-caused inhibition is abolished, Q_A⁻ reoxidation, controlled by the PSI-mediated reoxidation of PQH₂ to PQ, overcomes Q_A reduction; thus, unless much stronger actinic light could be used, complete closure of RCs is not achieved and F_P remains lower than F_M, practically at the F_I level. This has been indeed found in transients of preilluminated samples, and also in the presence of methylviologen that accepts electrons at the PSI acceptor side bypassing the block that inactive FNR creates. IP-phase also disappears in broken chloroplasts (the observed OJP transient is actually OJI), because ferredoxin is washed away during their isolation and electrons flow to other endogenous acceptor pools. (For a thorough investigation of the IP-phase, *see* Schansker *et al.* 2005).

The IP-phase disappears also when, for any reason, the electron flow to PSI acceptors is inhibited, but in that case it is the I-step that disappears as a distinct step, *i.e.*, F_I increases towards F_P = F_M; this was indeed found upon addition of dibromothymoquinone, which binds to the Cyt *b₆f* and inhibits the electron flow from PQH₂ to PC (Schansker *et al.* 2005). A limitation can also result from a stress that disconnects PSI from PSII, as found upon dehydration of *Haberlea rhodopensis* (Strasser *et al.* 2010).

The strongest evidence supporting the above interpretation of the JI- and IP-phases comes from the simultaneous recording of OJIP and the modulated reflection at 820 nm (MR₈₂₀, or simply MR) kinetics (Schansker *et al.* 2003, 2005). This evidence will be discussed here using the example presented in Fig. 7, which depicts both the OJIP (*closed points, left vertical axis*) and the MR = f(t) transients (*open points, right vertical axis*), recorded with the *M-PEA* instrument in dark-adapted leaves of the resurrection plant *H. rhodopensis* that were subjected to gradual water loss in darkness; the relative water content of the leaves (100, 26, and 10%) for each set is indicated. (Raw data were selected from Strasser *et al.* 2010). The modulated reflection signals are expressed as MR/MR₀, where MR₀ is the value at the onset of the actinic illumination (taken at 0.7 ms, the first reliable MR measurement).

Let us first focus on the control sample (*circles*; 100% RWC). The fast MR/MR₀ phase (decrease) ends at 7 ms. Thereafter and until ~ 30 ms, a transitory steady state at the minimum of MR/MR₀ follows. The fast decrease indicates the accumulation of P700⁺ and PC⁺, which cannot yet be reduced since PQ is still highly oxidised; this supports the interpretation of the OJ-phase (*see* subsection ‘Specific fluxes, quantum yields and other efficiencies’). The slowing down of the MR/MR₀ decrease indicates the beginning of some reduction of P700⁺ and PC⁺, being in good accordance with the initiation of the JI-phase. Notably, the highest rate of fluorescence increase (during the JI-phase) is at ~ 7 ms, when MR/MR₀ is entering the transitory steady state. This state, indicating equal oxidation and re-reduction rates of P700 and PC, is in the time range of the JI-phase and hence supports its

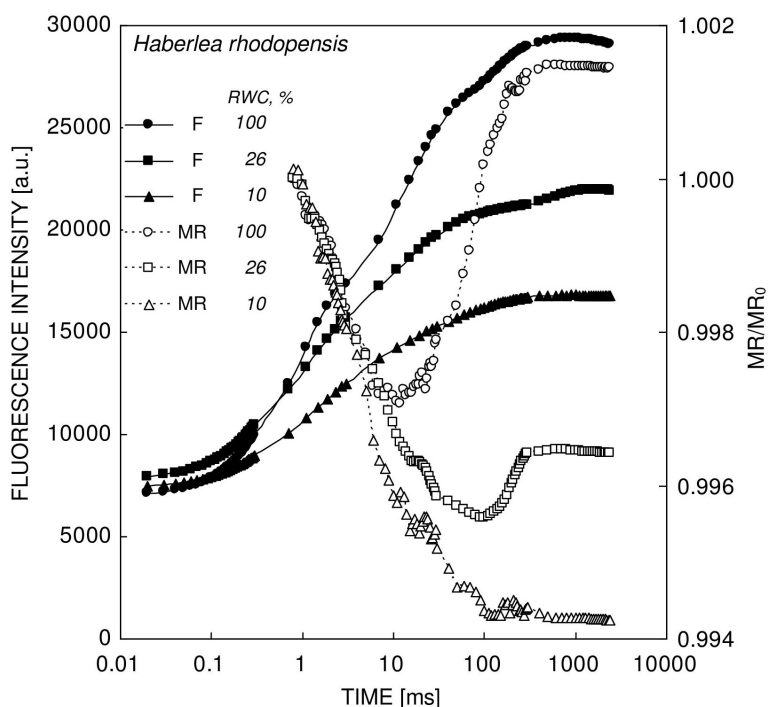


Fig. 7. OJIP fluorescence transients (closed markers, left vertical axis) and kinetics of modulated 820-nm reflection, MR/MR_0 (open markers, right vertical axis; MR_0 : the first reliable MR measurement, at 0.7 ms) induced by strong red actinic light [$5,000 \mu\text{mol}(\text{photon}) \text{m}^{-2} \text{s}^{-1}$; peak at 627 nm] and measured simultaneously with *M-PEA* in dark-adapted intact *Haberlea rhodopensis* leaves attached to the plants that were subjected to gradual water loss in darkness (relative water content, RWC, is indicated). (Raw data were obtained from Strasser *et al.* 2010).

interpretation as paralleling the net PQ reduction (with the reduction by Q_A^- predominating PQH_2 oxidation by PSI). The subsequent MR/MR_0 slow phase (increase) indicates the increasing net reduction of both $P700^+$ and PC^+ as, due to the bottleneck caused by inactive FNR, the available (oxidised) PSI electron acceptors are gradually exhausted, hence decelerating the PSI-mediated reoxidation of PC and $P700$. With $P700^+$ and PC^+ concentrations getting smaller, electron flow towards them slows down, PQ gets fully reduced and the P-level is reached at ~ 500 ms, when also the slow phase of MR/MR_0 levels off.

In conclusion, the finding that the MR/MR_0 slow phase corresponds, as above elucidated, to the IP-phase strongly supports the interpretation of the latter (see also Schansker *et al.* 2005). An additional support comes from the comparison of OJIP and $MR/MR_0 = f(t)$ obtained from *H. rhodopensis* leaves with different RWC (depicted in Fig. 7). Besides other effects that are not discussed here (see Strasser *et al.* 2010), the decrease of RWC exerts strong effects on the JI- and IP-phase and the MR/MR_0 transient in the same time range. At 26% RWC, compared to 100%, the fast MR/MR_0 phase is prolonged, indicating a slower reduction of $P700^+$ and PC^+ by PQH_2 . The shift of the initiation of the slow MR/MR_0 phase to longer times is accompanied by a similar shift of the initiation of the IP-phase, whose amplitude gets smaller. Moreover, MR/MR_0 slow phase attains a plateau at a lower level than that of the control sample, revealing that complete reduction of $P700^+$ and PC^+ cannot be achieved. At 10% RWC, the effects become more pronounced: the I-step disappears, the fast MR/MR_0 phase is further prolonged, while the slow phase does not develop at all. It was thus concluded that progressive drying disconnected gradually PSI from PSII (after PQH_2), with the findings from both

experimental approaches being in very good agreement, supplementing each other.

Parameters derived by the JIP-test

Based on the above analysed interpretations, the JIP-test was extended to include parameters related to the RE energy flux (Tsimilli-Michael and Strasser 2008b), as follows (see Fig. 6 and Appendix): the quantum yield of electron flux to PSI end electron acceptors is denoted as $\phi_{R_0} \equiv RE_0/ABS$. Since at I-step $dF_1/dt \cong 0$ (transitory steady state of Q_A^- concentration), the rate of Q_A^- reduction is equal (or can be approximated as equal) to the rate of Q_A^- reoxidation and, concomitantly, ϕ_{R_0} is equal to the quantum yield of primary photochemistry ϕ_{P_0} ; hence, application of Eq. 15 gives:

$$\begin{aligned} \phi_{R_0} \equiv RE_0/ABS &= \phi_{P_0} = \phi_{P_0} \times (1 - V_I) = \\ &= [1 - (F_0/F_M)] \times (1 - V_I) \end{aligned} \quad (29)$$

The efficiency/probability with which an electron from the intersystem electron carriers is transferred to reduce end electron acceptors at the PSI acceptor side is denoted as δ_{R_0} ; recalling Eq. 24, δ_{R_0} is given as:

$$\begin{aligned} \delta_{R_0} \equiv RE_0/ET_0 &= (RE_0/ABS)/(ET_0/ABS) = \phi_{R_0}/\phi_{E_0} = \\ &= [\phi_{P_0} \times (1 - V_I)]/[\phi_{P_0} \times (1 - V_J)] = (1 - V_I)/(1 - V_J) \end{aligned} \quad (30)$$

From Eqs. 21 and 30, the formula for the specific electron flux reducing PSI end electron acceptors is deduced:

$$\begin{aligned} RE_0/RC &= (RE_0/ET_0) \times (ET_0/RC) = \\ &= [(1 - V_I)/(1 - V_J)] \times (M_0/V_J) \times (1 - V_J) = \\ &= (1 - V_I) \times (M_0/V_J) \end{aligned} \quad (31)$$

Information obtained from the entire OJIP transient

The performance indexes PI_{ABS} and PI_{total} and the driving forces

The performance index PI_{ABS} was introduced as a product of terms expressing energy bifurcations from the absorption events to the reduction of the intersystem electron transport chain (Strasser *et al.* 2000, 2004), to be then extended as PI_{total} that incorporates also the energy bifurcation until the reduction of PSI end electron acceptors (Tsimilli-Michael and Strasser 2008b):

$$PI_{ABS} = \left(\frac{\gamma_{RC}}{1 - \gamma_{RC}} \right) \times \left(\frac{\phi_{P_0}}{1 - \phi_{P_0}} \right) \times \left(\frac{\psi_{E_0}}{1 - \psi_{E_0}} \right) \quad (32)$$

$$PI_{total} = \left(\frac{\gamma_{RC}}{1 - \gamma_{RC}} \right) \times \left(\frac{\phi_{P_0}}{1 - \phi_{P_0}} \right) \times \left(\frac{\psi_{E_0}}{1 - \psi_{E_0}} \right) \times \left(\frac{\delta_{R_0}}{1 - \delta_{R_0}} \right) \quad (33)$$

The parameter γ_{RC} is the probability that a PSII Chl *a* molecule functions as RC, *i.e.*,

$$\gamma_{RC} = \text{Chl}_{RC} / \text{Chl}_{\text{PSII-total}} = \text{RC} / (\text{ABS} + \text{RC}) \quad (34)$$

Hence, the term $\gamma_{RC}/(1 - \gamma_{RC})$ in Eqs. 32 and 33 is substituted by RC/ABS (*see* Appendix).

Substitution of the biophysical by experimental and basic parameters in Eq. 33 gives:

$$PI_{total} = \left(\frac{1 - F_0 / F_M}{M_0 / V_J} \right) \times \left(\frac{F_M - F_0}{F_0} \right) \times \left(\frac{1 - V_J}{V_J} \right) \times \left(\frac{1 - V_I}{V_I - V_J} \right) \quad (35)$$

As defined, the performance indexes are products of unitless $[p_i/(1 - p_i)]$ terms, where p_i ($i = 1, 2, \dots, n$) stands for probability (or fraction); hence, the terms express partial performances. Such expressions are well-known from Nernst's equation, where p_i is the fraction of the reduced and $(1 - p_i)$ the fraction of the oxidised form of a compound; in that case $\log[p_i/(1 - p_i)]$ expresses the potential or driving force for the corresponding oxidoreduction reaction. Extrapolating this inference from chemistry, the $\log(PI_{ABS})$ was defined (Strasser *et al.* 2004) as the total driving forces DF_{ABS} , which is the sum of partial driving forces:

$$DF_{ABS} = \log(PI_{ABS}) = \log\left(\frac{\text{RC}}{\text{ABS}}\right) + \log\left(\frac{\phi_{P_0}}{1 - \phi_{P_0}}\right) + \log\left(\frac{\psi_{E_0}}{1 - \psi_{E_0}}\right) \quad (36a)$$

Accordingly, the logarithm of PI_{total} is the total driving force DF_{total} :

$$DF_{total} = \log(PI_{total}) = \log\left(\frac{\text{RC}}{\text{ABS}}\right) + \log\left(\frac{\phi_{P_0}}{1 - \phi_{P_0}}\right) + \log\left(\frac{\psi_{E_0}}{1 - \psi_{E_0}}\right) + \log\left(\frac{\delta_{R_0}}{1 - \delta_{R_0}}\right) \quad (36b)$$

Since the calculated values of PI_{abs} and PI_{total} are on an arbitrary scale, they cannot be used to characterise a sample. It is their changes upon any environmental change/stress on any (but the same) photosynthetic material, that are meaningful. Hence the $[PI_{total}]/[PI_{total,control}]$ is mostly used and, accordingly, the $\Delta[DF_{total}] = [DF_{total}] - [DF_{total,control}]$.

The performance indexes, being obviously very sensitive parameters (especially PI_{total}), have proven to be very useful for routine screening of plants and evaluation of the overall impact of a stress on photosynthetic performance/behaviour, while their individual terms provide information for the impact on the sequential processes.

It is worth clarifying the following: (1) Though both PI_{ABS} and PI_{total} are determined from the kinetics of PSII fluorescence, PI_{total} evaluates impacts also on PSI behaviour (*via* the δ_{R_0} term). (2) When introduced, PI_{ABS} was denoted as 'performance index on absorption basis', hence the subscript 'ABS'. When the extended PI_{total} was defined, though it is also on absorption basis, it had to be distinguished; hence, subscript 'total' was used. (3) Like electrochemical potentials, driving forces DF_{ABS} and DF_{total} , as well as any partial DF, can be positive, negative or zero, since they are the logarithms of quantities that can be bigger, smaller or equal to unity.

Complementary Area and deduced parameters

Though used less frequently in JIP-test applications, the parameters Area and t_{F_M} (from the extracted data), the calculated S_m and the biophysical parameters EC_0/RC and turn-over number N , all obtained from the whole OJIP, merit explanation (*see* also Strasser *et al.* 2004).

The parameter Area (in ms), registered by all types of the *PEA*-instruments, is the total complementary area between the fluorescence induction curve and $F = F_P$ (meaningful only when $F_P = F_M$); it is hence given (and calculated if required) by the following formula, where t_{F_M} is the time needed to reach $F_P = F_M$:

$$\text{Area} = \int_0^{t_{F_M}} (F_M - F_t) dt \quad (37)$$

Normalization of Area on the maximum variable fluorescence, necessary to compare samples under different conditions, gives the parameter S_m (subscript 'm' stands for multiple-turnover events), which provides a measure of the excitation energy needed to be supplied (by open units) in order to close all RCs. It thus expresses a work-integral and also provides a measure of the amount (on an arbitrary scale) of all electron carriers reduced from time zero until t_{F_M} , denoted as EC_0/RC :

$$S_m \equiv \frac{1}{(F_M - F_0)} \int_0^{t_{F_M}} (F_M - F_t) dt = \int_0^{t_{F_M}} (1 - V_t) dt = EC_0 / \text{RC} \quad (38)$$

Accordingly, the normalised Area in DCMU-inhibited samples, denoted as S_s (subscript 's' for single-turnover event), would give a measure of the total amount of Q_A . Concomitantly, the ratio S_m/S_s expresses how many times

Q_A has been reduced from time zero to t_{F_M} and was hence denoted as turnover number, N . As addition of DCMU is not feasible in routine experiments, S_s can be taken, for *in vivo* conditions, as the inverse of the approximated (by Eq. 20) $M_{0,DCMU}$:

$$S_s = (M_{0,DCMU})^{-1} = V_J/M_0 \quad (39)$$

Hence,

$$N \equiv S_m/S_s = S_m \times (M_0/V_J) \quad (40)$$

Semiquantitative information from OJIP normalizations

The JIP-test was also extended to include the following ways for the comparison of a stressed sample with the non-stressed (control), with respect to the events reflected in the OJ, OI, JI, and IP phases (Strasser *et al.* 2004, 2007; Tsimilli-Michael and Strasser 2013b). The fluorescence kinetics $F_t = f(t)$ are normalized as V_t and as $W_{(YZ),t} = (F_t - F_Y)/(F_Z - F_Y)$, where Y and Z can be O and J, O and I, J and I, I and P; an additional useful normalization is between F_0 and $F_{300\mu s}$, as $W_{(O-300\mu s),t} \equiv (F_t - F_0)/(F_{300\mu s} - F_0)$. (Note: The general notation ‘W’ is commonly termed as [kind of] relative variable fluorescence).

Plotting the difference kinetics, $\Delta W_{(YZ),t} = [W_{(YZ),t} - [W_{(YZ),t}^{(control)}]]_t$, reveals bands that are usually hidden between the steps O, J, I, and P (Strasser *et al.* 2007). Hence, these subtractions provide a simple semiquantitative way to visualise the impact of stress; however, they should not be considered as providing additional information to those derived from the calculated parameters. The bands are interpreted as follows:

The difference kinetics $\Delta W_{(OJ),t}$ reveals the K-band, denoted so because its peak is at $\sim 300 \mu s$, where the K-step appears in the OKJIP transient (Strasser *et al.* 2004); moreover, when the above data processing was first introduced and this band was detected, it was attributed, like the K-step, to an inactivation of OEC that, if minor, would not be recognised in the raw fluorescence transient (*see* subsection ‘The K-step’). The K-band may also result from a bigger, compared to the control sample, functional PSII antenna size resulting in a steeper OJ rise (Yusuf *et al.* 2010, Tsimilli-Michael and Strasser 2013b). However, OEC inactivation results also in a lower P-step, while a bigger functional antenna does not affect it; this can be used as a criterion for deducing which of the two is reflected in the K-band, without excluding the possibility that they coexist, with a relative contribution that depends on stress severity.

The difference kinetics $\Delta W_{(O-300\mu s),t}$ reveals a band denoted as L-band, with peak at $\sim 100 \mu s$ (Strasser *et al.* 2007). As already written in this review (*see* subsection ‘Specific energy fluxes, quantum yields, and other efficiencies’), sigmoidal and exponential $W_{(OJ),t} = f(t)$ cross at $300 \mu s$. Hence, a positive L-band would reveal that stress resulted in a smaller p_G .

The difference kinetics $\Delta W_{(JI),t}$ reveals differences in the rate of net reduction of PQ. $\Delta W_{(OI),t}$ and ΔV_t exhibit a sequence of bands (except the L-band), including a band arising from differences with respect to the IP-phase.

Concerning the IP-phase, it is more informative to plot, in its time-range, the $W_{(OI),t} = f(t)$ and $W_{(IP),t} = f(t)$ for the samples/treatments to be compared (Yusuf *et al.* 2010). Fig. 8 presents an example, here of the beneficial effects of mycorrhization (as in Tsimilli-Michael and Strasser 2013b), which uses the average transients shown in Fig. 2. The increase of the $W_{(OI)}$ amplitude (insert of Fig. 8) indicates the beneficial effect on the relative size of electron acceptors’ pool at the PSI acceptor side and, moreover, that this effect is bigger in *Pinus brutia* than in *Pinus halepensis*. Comparison of the $W_{(IP),t} = f(t)$ kinetics (main plot of Fig. 8) provides an information not otherwise derived by the JIP-test, *i.e.*, whether the overall rate constant for reducing the certain pool, independently of possible effects on its size, is affected or not; here it shows that mycorrhization resulted in an increased rate only in the case of *Pinus brutia*.

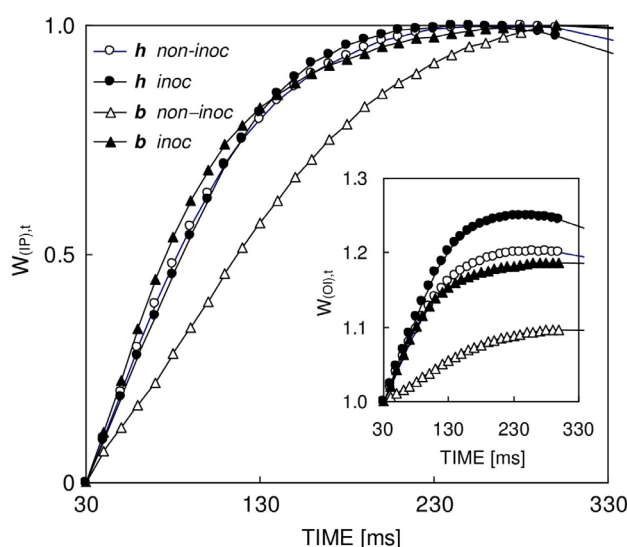


Fig. 8. The average Chl *a* fluorescence transients, depicted in Fig. 2, of dark-adapted needles of *Pinus halepensis* (*‘h’*, circles) and *Pinus brutia* (*‘b’*, triangles) trees grown in a gypsum quarry (in Cyprus), without (*open markers*) or with inoculation with a commercial mixture of ectomycorrhiza (*closed markers*), are expressed and plotted on a linear time scale in the range of the IP-phase as $W_{(IP),t} = (F_t - F_I)/(F_P - F_I) = f(t)$ in the main plot and $W_{(OI),t} = (F_t - F_O)/(F_I - F_O) = f(t)$ in the insert.

Epilogue

The JIP-test did not emerge out of ‘parthenogenesis’, as already stated in the Introduction, and has continued to get improved and extended since 1995 when it was first introduced. The simultaneous, with OJIP, recording of the modulated reflection at 820 nm has proven to be an important advancement, extending and supporting the JIP-test, as discussed above. Moreover, the simultaneous recording of delayed fluorescence (not included here; *see* Strasser *et al.* 2010) is a promising additional tool, as it will be that of the 515-nm absorbance changes on which Reto Strasser is presently working (personal communication).

JIP-test is not a 'bible', it is not the magic tool that reads and decodes nature. But, with its assumptions and approximations, as all models of nature need to adopt, it has been proven to be a powerful tool for what it is meant. It is powerful, by rapidly screening thousands of samples, for comparison and detection of stress effects; there are hundreds of publications on heat/drought/salinity/light-intensity/heavy-metals-contamination effects (that could not be cited here, given the aim of the review and the limited space available). There are also many publications on the detection and early diagnosis of beneficial effects, like those caused by mycorrhization (*e.g.*, Strasser *et al.* 2007, Tsimilli-Michael and Strasser 2008b, 2013b). It can also provide access to mechanisms, but cannot go further to elucidate them if it is not used together with other types of measurements, *e.g.*, of physiological parameters, chlorophyll content, gas-exchange data, modulated reflection at 820 nm.

Some last clarifications are deemed as necessary: (1) The many parameters of the JIP-test, being interlinked, do not carry as many independent pieces of information; however, the facility to calculate the whole set permits the choice of those that would better serve the needs of the investigation, as they recognise effects on specific semi-micro-transformers in the electron transport chain. (2) The JIP-test is meant to evaluate, by comparison, impacts of environmental factors/stressors on the photosynthetic structure and function, while the set of JIP-test parameters' values for a sample at a given physiological state is meaningless. (3) Accordingly, different species and/or mutants can be compared only by comparing the impact of the same stress on them but not by comparing their parameters' values at any given physiological state. (4) Though the JIP-test can be used to screen any type of stress, the biophysical meaning of the determined parameters is valid only when the stressed photosynthetic material is still within physiological limits.

It is hoped that the present review, with its analytical rederivations and clarifications will contribute to a better understanding of the JIP-test, which can help those who utilise it, both in applying it and in communicating their work between them. Moreover, parts of the review may be of interest and help also for readers who do not apply the JIP-test in their research.

References

- Delosme R.: [Studies on the induction of fluorescence in green algae and chloroplasts under intense illumination.] – *BBA-Bioenergetics* **143**: 108-128, 1967. [In French with English abstract]
- Duysens L.N.M., Sweers H.E.: Mechanism of the two photochemical reactions in algae as studied by means of fluorescence. – In: Japanese Society of Plant Physiologists (ed.): *Studies on Microalgae and Photosynthetic Bacteria*. Pp. 353-372. University of Tokyo Press, Tokyo 1963.
- Govindjee: Sixty-three years since Kautsky: Chlorophyll *a* fluorescence. – *Aust. J. Plant Physiol.* **22**: 131-160, 1995.
- Guissé B., Srivastava A., Strasser R.J.: Effects of high temperature and water stress on the polyphasic chlorophyll *a* fluorescence transient of potato leaves. – In: Mathis P. (ed.): *Photosynthesis: From Light to Biosphere*. Pp. 913-916. Kluwer Academic Publishers, Dordrecht 1995.
- Haldimann P., Strasser R.J.: Effects of anaerobiosis as probed by the polyphasic chlorophyll *a* fluorescence rise kinetic in pea (*Pisum sativum* L.). – *Photosynth. Res.* **62**: 67-83, 1999.
- Haldimann P., Tsimilli-Michael M.: Non-photochemical quenching of chlorophyll *a* fluorescence by oxidised plastoquinone: New evidences based on modulation of the redox state of the endogenous plastoquinone pool in broken spinach chloroplasts. – *BBA-Bioenergetics* **1706**: 239-249, 2005.
- Kautsky H., Hirsch A.: Neue Versuche zur Kohlensäure-assimilation. – *Naturwissenschaften* **19**: 964, 1931. [In German]
- Kitajima M., Butler W.L.: Quenching of chlorophyll fluorescence and primary photochemistry in chloroplasts by dibromothymoquinone. – *BBA-Bioenergetics* **376**: 105-115, 1975.
- Krüger G.H.J., Tsimilli-Michael M., Strasser R.J.: Light stress provokes plastic and elastic modifications in the structure and function of photosystem II in camellia leaves. – *Physiol. Plantarum* **101**: 265-277, 1997.
- Lazár D., Nauš J., Matoušková., Flašarová M.: Mathematical modelling of changes in chlorophyll fluorescence induction caused by herbicides. – *Pestic. Biochem. Phys.* **57**: 200-210, 1997.
- Neubauer C., Schreiber U.: The polyphasic rise of chlorophyll fluorescence upon onset of strong continuous illumination: 1. Saturation characteristics and partial control by the photosystem II acceptor side. – *Z. Naturforsch.* **42c**: 1246-1254, 1987.
- Paillotin G.: Movement of excitations in the photosynthetic domains of photosystem II. – *J. Theor. Biol.* **58**: 237-252, 1976.
- Papageorgiou G.C., Govindjee (ed.): *Chlorophyll *a* Fluorescence: A Signature of Photosynthesis: Advances in Photosynthesis and Respiration*, Vol. 19. Pp. 820. Springer, Dordrecht 2004.
- Schansker G., Srivastava A., Govindjee, Strasser R.J.: Characterization of 820 nm transmission signal paralleling the chlorophyll *a* fluorescence rise (OJIP) in pea leaves. – *Funct. Plant Biol.* **30**: 785-796, 2003.
- Schansker G., Tóth S.Z., Holzwarth A.R., Garab G.: Chlorophyll *a* fluorescence: Beyond the limit of the Q_A model. – *Photosynth. Res.* **120**: 43-58, 2014.
- Schansker G., Tóth S.Z., Strasser R.J.: Methylviologen and dibromothymoquinone treatments of pea leaves reveal the role of photosystem I in the Chl *a* fluorescence rise OJIP. – *BBA-Bioenergetics* **1706**: 250-261, 2005.
- Srivastava A., Guissé B., Greppin H., Strasser R.J.: Regulation of antenna structure and electron transport in PS II of *Pisum sativum* under elevated temperature probed by the fast polyphasic chlorophyll *a* fluorescence transient: OKJIP. – *BBA-Bioenergetics* **1320**: 95-106, 1997.
- Stirbet A.D., Srivastava A., Strasser R.J.: The energetic connectivity of PS II centers in higher plants probed *in vivo* by the fast fluorescence rise O-J-I-P and numerical simulations. – In: Garab G. (ed.): *Photosynthesis: Mechanisms and Effects*. Pp. 4317-4320. Kluwer Academic Publishers, Dordrecht 1998.
- Strasser B.J., Strasser R.J.: Measuring fast fluorescence transients to address environmental questions: The JIP-test. – In: Mathis P. (ed.): *Photosynthesis: From Light to Biosphere*. Pp. 977-980. Kluwer Academic Publishers, Dordrecht 1995.
- Strasser R.J.: The grouping model of plant photosynthesis. – In: Akoyunoglou G., Argyroudi-Akoyunoglou J.H. (ed.): *Chloroplast Development*. Pp. 513-524. Elsevier, Amsterdam 1978.
- Strasser R.J.: The grouping model of plant photosynthesis: heterogeneity of photosynthetic units in thylakoids. –

- In: Akoyunoglou G. (ed.): Photosynthesis III. Structure and Molecular Organisation of the Photosynthetic Apparatus. Pp. 727-737. Balaban International Science Services, Philadelphia 1981.
- Strasser R.J., Govindjee: The F_0 and the O-J-I-P fluorescence rise in higher plants and algae. – In: Argyroudi-Akoyunoglou J.H. (ed.): Regulation of Chloroplast Biogenesis. Pp. 423-426. Plenum Press, New York 1992.
- Strasser R.J., Srivastava A., Govindjee: Polyphasic chlorophyll *a* fluorescence transient in plants and cyanobacteria. – Photochem. Photobiol. **61**: 32-42, 1995.
- Strasser R.J., Srivastava A., Tsimilli-Michael M.: The fluorescence transient as a tool to characterize and screen photosynthetic samples. – In: Yunus M., Pathre U., Mohanty P. (ed.): Probing Photosynthesis: Mechanism, Regulation and Adaptation. Pp. 443-480. Taylor and Francis, London 2000.
- Strasser R.J., Stirbet A.D.: Estimation of the energetic connectivity of PS II centres in plants using the fluorescence rise O-J-I-P. Fitting of experimental data to three different PS II models. – Math. Comput. Simulat. **56**: 451-461, 2001.
- Strasser R.J., Tsimilli-Michael M.: Activity and heterogeneity of PS II probed *in vivo* by the chlorophyll *a* fluorescence rise O-(K)-J-I-P. – In: Garab G. (ed.): Photosynthesis: Mechanisms and Effects. Pp. 4321-4324. Kluwer Academic Publishers, Dordrecht 1998.
- Strasser R.J., Tsimilli-Michael M., Dangre D., Rai M.: Biophysical phenomics reveals functional building blocks of plants systems biology: A case study for the evaluation of the impact of mycorrhization with *Piriformospora indica*. – In: Varma A., Oelmüller R. (ed.): Advanced Techniques in Soil Microbiology. Soil Biology. Vol. 11. Pp. 319-342. Springer-Verlag, Berlin 2007.
- Strasser R.J., Tsimilli-Michael M., Qiang S., Goltsev V.: Simultaneous *in vivo* recording of prompt and delayed fluorescence and 820-nm reflection changes during drying and after rehydration of the resurrection plant *Haberlea rhodopensis*. – BBA-Bioenergetics **1797**: 1313-1326, 2010.
- Strasser R.J., Tsimilli-Michael M., Srivastava A.: Analysis of the chlorophyll *a* fluorescence transient. – In: Papageorgiou G.C., Govindjee (ed.): Chlorophyll *a* Fluorescence: A Signature of Photosynthesis. Advances in Photosynthesis and Respiration. Pp. 321-362. Springer, Dordrecht 2004.
- Tsimilli-Michael M., Jarraud N., Strasser R.J.: Reforestation in Cyprus – *in vivo* and *in situ* assessment of mycorrhization impact on plants' vitality with the JIP-test. – In: Proceedings of the COST Action 870 Meeting 'Mycorrhiza Application in Sustainable Agriculture and Natural Systems'. Pp. 76-79. Thessaloniki, Greece 2008.
- Tsimilli-Michael M., Stamatakis K., Papageorgiou G.C.: Dark-to-light transition in *Synechococcus* sp. PCC 7942 cells studied by fluorescence kinetics assesses plastoquinone redox poise in the dark and photosystem II fluorescence component and dynamics during state 2 to state 1 transition. – Photosynth. Res. **99**: 243-255, 2009.
- Tsimilli-Michael M., Strasser R.J.: Experimental resolution and theoretical complexity determine the amount of information extractable from the chlorophyll fluorescence transient OJIP. – In: Allen J.F., Gantt E., Golbeck J.H., Osmond B. (ed.): Photosynthesis. Energy from the Sun. Pp. 697-701. Springer Dordrecht 2008a.
- Tsimilli-Michael M., Strasser R.J.: *In vivo* assessment of stress impact on plants' vitality: applications in detecting and evaluating the beneficial role of mycorrhization on host plants. – In: Varma A. (ed.): Mycorrhiza. State of the Art, Genetics and Molecular Biology, Eco-Function, Biotechnology, Eco-Physiology, Structure and Systematics. 3rd edition. Pp. 679-703. Springer, Berlin-Heidelberg 2008b.
- Tsimilli-Michael M., Strasser R.J.: The energy flux theory 35 years later: Formulations and applications. – Photosynth. Res. **117**: 289-320, 2013a.
- Tsimilli-Michael M., Strasser R.J.: Biophysical phenomics: Evaluation of the impact of mycorrhization with *Piriformospora indica*. – In: Varma A., Kost G., Oelmüller R. (ed.): *Piriformospora indica*. Sebasinales and Their Biotechnological Applications. Pp. 173-190. Springer-Verlag, Berlin-Heidelberg 2013b.
- Vredenberg W.J.: A three-state model for energy trapping and chlorophyll fluorescence in photosystem II incorporating radical pair recombination. – Biophys. J. **79**: 26-38, 2000.
- Yusuf M.A., Kumar D., Rajwanshi R. *et al.*: Overexpression of γ -tocopherol methyl transferase gene in transgenic *Brassica juncea* plants alleviates abiotic stress: Physiological and chlorophyll *a* fluorescence measurements. – BBA-Bioenergetics **1797**: 1428-1438, 2010.

Appendix. Glossary, definition of terms, and formulae used by the JIP-test for the analysis of the Chl *a* fluorescence transient OJIP emitted by dark-adapted photosynthetic samples (modified after Strasser *et al.* 2004 with extensions from Tsimilli-Michael and Strasser 2008b). Subscript '0' (or 'o') indicates that a parameter refers to the starting conditions. Symbol 'F' denoted as 'fluorescence', means fluorescence intensity.

DATA EXTRACTED FROM THE RECORDED FLUORESCENCE TRANSIENT OJIP

F_t	fluorescence at time <i>t</i> after onset of actinic illumination
$F_{50\mu s}$ or $F_{20\mu s}$	minimal reliable recorded fluorescence, at 50 μs with the <i>PEA</i> instrument or 20 μs with <i>Handy-</i> , <i>Pocket-</i> , <i>Senior-</i> , and <i>M-PEA</i>
$F_{50\mu s}$	fluorescence at 50 μs (for the calculation of the slope)
$F_{100\mu s}$	fluorescence at 100 μs (for the calculation of p_G)
$F_{300\mu s}$	fluorescence at 300 μs
$F_J \equiv F_{2ms}$	fluorescence at the J-step (2 ms) of OJIP
$F_I \equiv F_{30ms}$	fluorescence at the I-step (30 ms) of OJIP
F_P	maximal recorded fluorescence, at the peak P of OJIP
t_{F_M}	time (in ms) to reach the maximal fluorescence F_P (meaningful only when $F_P = F_M$)
Area	total complementary area between the fluorescence induction curve and $F = F_P$ (meaningful only when $F_P = F_M$)

BASIC PARAMETERS CALCULATED FROM THE EXTRACTED DATA

$F_0 \cong F_{50\mu s}$ or $\cong F_{20\mu s}$	fluorescence when all PSII RCs are open (\cong to the minimal reliable recorded fluorescence)
$F_M (= F_P)$	maximal fluorescence, when all PSII RCs are closed (= F_P when the actinic light intensity is above $500 \mu\text{mol}(\text{photon}) \text{m}^{-2} \text{s}^{-1}$ and provided that all RCs are active as Q_A -reducing)
$F_v \equiv F_t - F_0$	variable fluorescence at time t
$F_V \equiv F_M - F_0$	maximal variable fluorescence
$V_t \equiv F_v/F_V \equiv (F_t - F_0)/(F_M - F_0)$	relative variable fluorescence at time t (normalisation on $F_M - F_0$)
$W_{(YZ),t} \equiv (F_t - F_Y)/(F_Z - F_Y)$	different types of relative variable fluorescence at time t, with $(F_Z - F_Y)$ standing for $(F_{300\mu s} - F_0)$, or $(F_J - F_0)$, or $(F_I - F_J)$, or $(F_I - F_0)$, or $(F_P - F_I)$
$M_0 \equiv [(\Delta F/\Delta t)_0]/(F_M - F_0)$ $\equiv 4 \times (F_{300\mu s} - F_{50\mu s})/(F_M - F_0)$ $\equiv 4 \times (V_{300\mu s} - V_{50\mu s})$	approximated initial slope (in ms^{-1}) of the fluorescence transient normalised on the maximal variable fluorescence $F_M - F_0 = F_V$; equivalently, initial slope (50 to 300 μs ; in ms^{-1}) of the $V_t = f(t)$ kinetics
$S_m \equiv \text{Area}/(F_M - F_0) = \text{Area}/F_V$	normalised Area

BIOPHYSICAL PARAMETERS DERIVED FROM THE BASIC PARAMETERS BY THE JIP-TEST

Deexcitation rate constants of PSII antenna

$k_N = (\text{ABS}) \times k_F \times (1/F_M)$	nonphotochemical deexcitation rate constant (ABS: absorption flux – see below; k_F : rate constant for fluorescence emission)
$k_P = (\text{ABS}) \times k_F \times (1/F_0 - 1/F_M) = k_N \times (F_V/F_0)$	photochemical deexcitation rate constant

Specific energy fluxes (per RC: Q_A -reducing PSII reaction centre), in ms^{-1}

$\text{ABS}/\text{RC} = M_0 \times (1/V_J) \times (1/\phi_{P_0})$	absorption flux (exciting PSII antenna Chl <i>a</i> molecules) per RC (also used as a unit-less measure of PSII apparent antenna size)
$\text{TR}_0/\text{RC} = M_0 \times (1/V_I)$	trapped energy flux (leading to Q_A reduction), per RC
$\text{ET}_0/\text{RC} = M_0 \times (1/V_J) \times (1 - V_J)$	electron transport flux (further than Q_A^-), per RC
$\text{RE}_0/\text{RC} = M_0 \times (1/V_J) \times (1 - V_I)$	electron flux reducing end electron acceptors at the PSI acceptor side, per RC

Quantum yields and efficiencies

$\phi_{P_t} \equiv \text{TR}_t/\text{ABS} = [1 - (F_t/F_M)] = \Delta F_t/F_M$	quantum yield for primary photochemistry at any time t
$\phi_{P_0} \equiv \text{TR}_0/\text{ABS} = [1 - (F_0/F_M)]$	maximum quantum yield for primary photochemistry
$\phi_{E_0} \equiv \text{ET}_0/\text{ABS} = [1 - (F_0/F_M)] \times (1 - V_J)$	quantum yield for electron transport (ET)
$\phi_{R_0} \equiv \text{RE}_0/\text{ABS} = [1 - (F_0/F_M)] \times (1 - V_I)$	quantum yield for reduction of end electron acceptors at the PSI acceptor side (RE)
$\psi_{E_0} \equiv \text{ET}_0/\text{TR}_0 = (1 - V_J)$	efficiency/probability that an electron moves further than Q_A^-
$\delta_{R_0} \equiv \text{RE}_0/\text{ET}_0 = (1 - V_I)/(1 - V_J)$	efficiency/probability with which an electron from the intersystem electron carriers is transferred to reduce end electron acceptors at the PSI acceptor side (RE)

Other biophysical parameters

$\text{EC}_0/\text{RC} = S_m \equiv \text{Area}/F_V$	a measure of total electron carriers, per RC, reduced from time zero until t_{F_M}
$N = S_m \times (M_0/V_J)$	turnover number (expresses how many times Q_A is reduced in the time interval from 0 to t_{F_M})
p_G (see Eq. 28)	grouping probability (between PSII units)
$\gamma_{\text{RC}} = \text{Chl}_{\text{RC}}/\text{Chl}_{\text{PSII-total}} = \text{RC}/(\text{ABS} + \text{RC})$	probability that a PSII Chl <i>a</i> molecule functions as RC
$\text{RC}/\text{ABS} = \gamma_{\text{RC}}/(1 - \gamma_{\text{RC}}) = \phi_{P_0} \times (V_J/M_0) = (\text{ABS}/\text{RC})^{-1}$	RCs per PSII antenna Chl <i>a</i> (reciprocal of ABS/RC)

Performance indexes

$\text{PI}_{\text{ABS}} \equiv \frac{\gamma_{\text{RC}}}{1 - \gamma_{\text{RC}}} \times \frac{\phi_{P_0}}{1 - \phi_{P_0}} \times \frac{\psi_{E_0}}{1 - \psi_{E_0}}$	performance index for energy conservation from photons absorbed by PSII until the reduction of intersystem electron acceptors
$\text{PI}_{\text{total}} \equiv \text{PI}_{\text{ABS}} \times \frac{\delta_{R_0}}{1 - \delta_{R_0}}$	performance index for energy conservation from photons absorbed by PSII until the reduction of PSI end electron acceptors

Driving forces (logarithms of performance indexes)

$$DF_{\text{ABS}} \equiv \log(\text{PI}_{\text{ABS}}) =$$

$$= \log \frac{\gamma_{\text{RC}}}{1 - \gamma_{\text{RC}}} + \log \frac{\phi_{\text{Pb}}}{1 - \phi_{\text{Pb}}} + \log \frac{\psi_{\text{Eo}}}{1 - \psi_{\text{Eo}}}$$

driving force (potential) for energy conservation from photons absorbed by PSII until the reduction of intersystem electron acceptors

$$DF_{\text{total}} \equiv \log(\text{PI}_{\text{total}}) = DF_{\text{ABS}} + \log \frac{\delta_{\text{Ro}}}{1 - \delta_{\text{Ro}}}$$

driving force (potential) for energy conservation from photons absorbed by PSII until the reduction of PSI end electron acceptors

© The authors. This is an open access article distributed under the terms of the Creative Commons BY-NC-ND Licence.